AD NUMBER
AD044243
LIMITATION CHANGES
TO: **Approved for public release; distribution is unlimited.**
FROM: **Distribution authorized to U.S. Gov't. agencies and their contractors; Administrative/Operational Use; FEB 1954. Other requests shall be referred to Naval Ordnance Systems Command, Washington, DC 20360.**
AUTHORITY
usnol ltr, 29 aug 1974

NAVORD REPORT 3596

PRELIMINARY ANALYSIS OF THE HALF-WAVE BRIDGE MAGNETIC AMPLIFIER

12 FEBRUARY 1954

U. S. NAVAL ORDNANCE LABORATORY
WHITE OAK, MARYLAND

PRELIMINARY ANALYSIS OF THE HALF-WAVE BRIDGE MAGNETIC AMPLIFIER

Prepared by:

H. H. Woodson

ABSTRACT: Two half-wave bridge magnetic amplifiers -- one with parallel reset circuits, the other with series reset circuits -- are analyzed using only linear circuit theory and Faraday's Law. The principal assumptions used in the analysis are rectangular B-H loop reactor core material and resistive rectifier impedances. The results of the analysis are discussed with particular emphasis on the effect the various circuit parameters have on the amplifier gain. Some design criteria are established and theoretically justified. The extensions of this type of analysis to other than the half-wave bridge circuit are indicated.

U. S. NAVAL ORDNANCE LABORATORY
White Oak, Maryland

NAVORD Report 3596 12 February 1954

The use of the half-wave bridge magnetic amplifier in high performance servo systems has proved practical. Optimum design of this amplifier is best achieved if the operation is described quantitatively in such a manner that the effect of each individual component on the amplifier gain is apparent.

Under the Magnetic Amplifier Development Program, NOL-A8f-1-2-54, and the Magnetic Amplifier Servo System Development Program, NOL-B4a-78-2-54, a quantitative analysis was started which gave the information desired. This report covers the preliminary part of this analysis. Further detailed analysis and experimental checks will be given as they are completed.

EDWARD L. WOODYARD
Captain, USN
Commander

D. S. Muzzey, Jr.

D. S. MUZZEY, JR.
By direction

CONTENTS

ILLUSTRATIONS

PRELIMINARY ANALYSIS OF THE HALF-WAVE BRIDGE MAGNETIC AMPLIFIER

INTRODUCTION

1. The application of the half-wave bridge magnetic amplifier[1,2,3] to high-performance servo systems has been quite successful. This success is attributable to a number of advantages this circuit has when compared to other types of servo amplifiers. The principal advantages of the half-wave bridge compared to vacuum tube amplifiers are ruggedness and reliability, and ease and simplicity of compensation.[4,5,6,7] Compared to conventional full-wave magnetic amplifier circuits the half-wave bridge magnetic amplifier has the advantages of fast response[1,3] and ease and simplicity of compensation.

2. When the half-wave bridge magnetic amplifier was first used the design of an amplifier for a specific application was achieved through the use of past experience and cut-and-try procedures. A partial solution to this difficulty was obtained when a good qualitative design procedure was developed at the Naval Ordnance Laboratory. This design procedure, presented in reference (3), pointed out the significant parameters to be adjusted for best operation and gave the method of adjustment. Being qualitative, this design procedure still left some adjustments to engineering judgment.

3. The analysis in the present report is intended to supplement the design procedure given in reference (3). This is achieved by using the same fundamental approach as in this reference, but the circuit is examined in greater quantitative detail.

DESCRIPTION OF CIRCUITS

4. The half-wave bridge magnetic amplifier circuits to be analyzed are shown in figures 1(a) and 1(b). The only difference between the circuits is in the configuration of the reset circuits. The bridge of figure 1(a) has parallel reset circuits, while the bridge of figure 1(b) has series reset circuits. The differences in the operation of the two circuits will be made evident in the analysis to follow.

5. Each of the circuits of figure 1 employs two saturable reactors. One reactor has power windings N_1 and N_3, reset windings N_{r_1}, and control winding N_{c_1}; while the other reactor has power windings N_2 and N_4, reset winding N_{r_2}, and control winding N_{c_2}. Note that all windings with odd subscripts are on one reactor while all with even subscripts are on the other reactor.

6. Briefly the half-wave bridge circuit operates as follows. The bridge stays balanced under zero signal conditions because during the reset half-cycle (when the supply voltage has the opposite polarity to that shown in figure 1) the flux change from saturation, produced by voltage across windings N_{r_1} and N_{r_2}, is the same. As a result, during the operating half-cycle (when the supply voltage has the polarity shown in figure 1) both reactors reach saturation at the ssme time maintaining zero load current. A control voltage, v_c, applied to the differentially connected control windings N_{c_1} and N_{c_2} will produce a difference in flux between the two reactors during the reset half-cycle. This flux difference causes the reactors to saturate at different times during the next operating half-cycle. During the interval of time when one reactor is saturated and the other is unsaturated, current will flow through the load resistance R_L. The direction of load current flow is determined by the polarity of the control voltage.

7. The presence of the rectifiers in the circuit makes the conditions different during the reset and operating half-cycles; consequently, these two modes of operation must be considered separately. Before the analysis can be started, however, assumptions must be made regarding the nonlinearities in the circuit.

ASSUMPTIONS

8. Each of the reactors is assumed to be a four terminal-pair network with a number of turns associated with each terminal pair as shown in figure 2*. This network is assumed to have two modes of operation. If the external circuits can supply sufficient current and the core flux level, ϕ, satisfies the relation

$$|\phi| < |\phi_s| \qquad (1)$$

where ϕ_s is the saturation flux of the core; then the following two relations describe the operation of the reactor:

$$\frac{e_1}{N_1} = \frac{e_2}{N_2} = \frac{e_r}{N_r} = \frac{e_c}{N_c}, \qquad (2)$$

and

$$N_1 i_1 + N_2 i_2 + N_r i_r + N_c i_c = (NI)_s \qquad (3)$$

* The d-c resistances of the windings are lumped with the external circuits.

where (NI) is the coercive ampere-turns of the core. To maintain accuracy in design this coercive force must be measured under the approximate conditions to be analyzed, i.e. at the line frequency to be used and operating about a minor loop. If the external circuits cannot supply sufficient current to satisfy equation (3), or if the core flux ϕ equals the saturation value $\pm \phi_s$, each pair of terminals of the network of figure 2 is short-circuited with no mutual coupling between terminal pairs. The above characteristics describe a reactor with the flux ampere-turns loop shown in figure 3 with

$$\phi = \frac{1}{N_1}\int_{-\infty}^{t} e_1\,dt = \frac{1}{N_2}\int_{-\infty}^{t} e_2\,dt = \frac{1}{N_r}\int_{-\infty}^{t} e_r\,dt = \frac{1}{N_c}\int_{-\infty}^{t} e_c\,dt, \qquad (4)$$

and

$$(Ni) = N_1 i_1 + N_2 i_2 + N_r i_r + N_c i_c. \qquad (5)$$

If the loop is crossed at any flux level, the operating path is at constant flux as shown by path a-b in figure 3. The winding resistances are lumped with the external circuits and the leakage reactances are assumed zero, a good assumption with toroidal reactors. The above assumptions concerning reactor characteristics are quite accurate for a reactor using a rectangular-loop core material such as Orthonol.

9. The rectifiers are assumed to have the equivalent circuit shown in figure 4, where the rectifier, RX, is perfect (zero forward impedance, infinite reverse impedance) and R_{f_1} and R_R are the constant forward and reverse resistances respectively. There are two sources of error in these assumptions. First, the forward and reverse resistances are not constant; however, when the values are measured as average values under a-c operation at approximately the frequency, voltage, and current levels occurring in the amplifier circuit, the errors will not be intolerable. Second, selenium rectifiers exhibit a capacitive reverse impedance; thus, the error due to capacitive reverse current increases with increasing line frequency. The addition of an equivalent capacitance to the circuit of figure 4 complicates the analysis to follow, and the analysis neglecting the capacitance is sufficiently correct; consequently, capacitance of the rectifier is neglected. Of course, if germanium diodes are used, the capacitance is negligible and the equivalent circuit of figure 4 becomes a better approximation.

10. All other components in the circuits of figure 1 are assumed to be resistive.

ANALYSIS FOR QUIESCENT CONDITIONS
(Complete Analysis in Appendices A, B and C)

11. In the design of an amplifier for a given application, a knowledge of the quiescent operation is desired for two reasons. First, the "firing angle" (the angle during the operating half-cycle at which the reactors saturate) must be adjusted to provide the proper phasing of the fundamental frequency component of the output voltage to provide optimum control of a two-phase servo motor or to place the output pulse at the position in the operating half-cycle to give optimum control of a succeeding cascaded amplifier stage. Second, the quiescent power will be limited by the specified allowable temperature rise in the amplifier.

12. The quiescent "firing angle", ωt_3, for the bridge of figure 1(a) with parallel reset is given by equation (C11) of Appendix C:

$$\omega t_3 = \cos^{-1}\left\{1 - \frac{4\frac{N_s}{N_r}\left(1+\frac{N_s}{N_r}\frac{R_b}{R_R}\right)}{1+2\left(\frac{N_s}{N_r}\right)^2\frac{R_b}{R_R}}\left(\cos\sin^{-1}\alpha_o - \alpha_o\cos^{-1}\alpha_o\right)\right\}, \qquad (6)$$

while the quiescent "firing angle" for the bridge of figure 1(b) with series reset is given by equation (C12) of Appendix C:

$$\omega t_3 = \cos^{-1}\left\{1 - \frac{2\frac{N_s}{N_r}\left(1+\frac{N_s}{N_r}\frac{R_b}{R_R}\right)}{1+\left(\frac{N_s}{N_r}\right)^2\frac{R_b}{R_R}}\left(\cos\sin^{-1}\alpha_o - \alpha_o\cos^{-1}\alpha_o\right)\right\}. \qquad (7)$$

In equations (6) and (7) the factor α_o is given by equation (A13) of Appendix A as:

$$\alpha_o = \frac{\frac{R_b(NI)}{N_r V_s}}{1+\frac{N_s}{N_r}\frac{R_b}{R_R}}. \qquad (8)$$

In the above expressions:

N_r = Number of turns on reset winding

N_s = Number of turns on one power winding

R_b = Resistance of reset circuit

R_R = Reverse resistance of one power circuit rectifier

V_s = Amplitude of supply voltage

ω = Angular frequency of supply voltage

(NI) = Coercive mmf of reactors.

13. In the design of an amplifier for a particular application the power winding turns, N_s, rectifier reverse resistance, R_R, and coercive mmf (NI) are determined from load considerations[3], i.e. power requirements and impedance level*.

14. The parameters remaining for adjustment of the "firing angle" are the reset resistance, R_b, and the reset turns, N_r. After the proper firing angle has been chosen, the values of R_b and N_r are set by gain considerations to be discussed later, using either equation (6) or (7) as a constraint on R_b and N_r, depending on whether parallel or series reset is used.

15. The considerations discussed above determine all the parameter values in the expression of equation (6) or (7). Thus, control over the quiescent power must be exercised with some parameter other than those given in these equations. The average quiescent power, P_q, is given by equation (C6) of Appendix C as:

$$P_q = \frac{1}{2\pi} \frac{V_s^2}{(R_s + R_f)} (\pi - \omega t_3 + \sin \omega t_3 \cos \omega t_3) \qquad (9)$$

where R_s = Series resistance in line

R_f = Saturated forward impedance of one arm of power circuit

and the firing angle ωt_3 is given by equation (6) for a bridge with parallel reset or equation (7) for a bridge with series reset. Since all the parameters determining the firing angle, ωt_3, have already been determined, the only parameters left for adjustment of the quiescent power are the resistances R_s and R_f. In the treatment of gain to be given subsequently it will be shown that the gain is not affected by the line resistance R_s, while it is affected by the saturated impedance of the bridge R_f; consequently, the line resistance R_s can be used to limit the quiescent power dissipated in the bridge while not affecting the gain of the stage.

* The fact that load considerations fix rectifier reverse resistance may not be readily obvious because the rectifier forward impedance is the parameter primarily fixed by load considerations. The type of rectifier (selenium, germanium, etc.) to be used is chosen from operating conditions (temperature, voltage, etc.) and for any type of rectifier the reverse resistance varies nearly in direct proportion to the forward resistance.

ANALYSIS FOR SIGNAL CONDITIONS*
(Complete Analysis in Appendices D, E, F, G and H)

16. For the half-wave bridge circuit with parallel reset circuits of figure 1(a) the average load voltage, V_L, as a function of the direct control voltage, V_c, is given by equation (G1) of Appendix G:

$$V_L = \left(\frac{R_L}{R_L + R_f}\right)\left[\frac{K_1 N_c}{R_c + K_1 N_c^2}\,\frac{N_s V_c}{\pi}\cos^{-1}(\alpha_0 + \alpha_2 V_c)\right.$$

$$+\frac{N_s}{N_p}\,\frac{V_s}{2\pi}\,\frac{1+\frac{N_s}{N_p}\frac{R_b}{R_R}}{1+\left(\frac{N_s}{N_p}\right)^2\frac{R_b}{R_R}+2\left(\frac{N_s}{N_p}\right)^2\frac{R_b}{R_R}}\left\{\cos\sin^{-1}(\alpha_0-\alpha_1 V_c)\right.$$

$$-\cos\sin^{-1}(\alpha_0+\alpha_2 V_c)+\left(\frac{\frac{N_s}{N_p}\frac{R_b}{R_c}\frac{V_c}{V_s}}{1+\frac{N_s}{N_p}\frac{R_b}{R_R}}-\alpha_0\right)\left[\sin^{-1}(\alpha_0+\alpha_2 V_c)\right.$$

$$\left.\left.\left.-\sin^{-1}(\alpha_0-\alpha_1 V_c)\right]\right\}\right], \qquad (10)$$

where α_0 is given by equation (8) and α_1, α_2, and K_1 are given by equations (D8), (D19), and (D34) of Appendix D thus:

$$\alpha_1 = \frac{\frac{N_s}{N_p}\frac{R_b}{R_c}\frac{1}{V_s}}{1+\frac{N_s}{N_p}\frac{R_b}{R_R}}, \qquad (11)$$

* The analysis in this report is carried out for a direct control voltage; however, any control voltage which is a specified periodic time function with the period equal to the period of the supply voltage can be used. The modifications that need to be made in the analysis for such a voltage are evident in the form of the analysis.

$$\alpha_2 = \frac{\frac{N_c}{N_r}\frac{R_b}{R_c}\frac{1}{V_s}\left[1+2\left(\frac{N_s}{N_r}\right)^2\frac{R_b}{R_R}\right]}{\left(1+\frac{N_s}{N_r}\frac{R_b}{R_R}\right)\left[1+2\left(\frac{N_c}{N_r}\right)^2\frac{R_b}{R_c}+2\left(\frac{N_s}{N_r}\right)^2\frac{R_b}{R_R}\right]}, \tag{12}$$

$$K_1 = \frac{2}{\frac{N_r^2}{R_b}+2\frac{N_s^2}{R_R}}. \tag{13}$$

17. For the bridge with series reset circuits of figure 1(b) the average load voltage as a function of the direct control voltage is from equation (H1) of Appendix H:

$$V_L = \left(\frac{R_L}{R_L+R_f}\right)\left[\frac{K_2 N_c}{R_c+K_2 N_c^2}\frac{N_s V_c}{\pi}\cos^{-1}(\alpha_0+\alpha_3 V_c)\right.$$

$$+\frac{N_s}{N_r}\frac{V_s}{2\pi}\frac{1+\frac{N_s}{N_r}\frac{R_b}{R_R}}{1+\left(\frac{N_s}{N_r}\right)^2\frac{R_b}{R_c}+2\left(\frac{N_s}{N_r}\right)^2\frac{R_b}{R_R}}\left\{\cos\sin^{-1}(\alpha_0-\alpha_1 V_c)\right.$$

$$-\cos\sin^{-1}(\alpha_0+\alpha_3 V_c)+\left(\frac{\frac{N_c}{N_r}\frac{R_b}{R_c}\frac{V_c}{V_s}}{1+\frac{N_s}{N_r}\frac{R_b}{R_R}}-\alpha_0\right)\left[\sin^{-1}(\alpha_0+\alpha_3 V_c)\right.$$

$$\left.\left.\left.-\sin^{-1}(\alpha_0-\alpha_1 V_c)\right]\right\}\right], \tag{14}$$

where α_0 is given by equation (8), α_1 is given by equation (11) and α_3 and K_2 are given by equation (E18) and (E31) of Appendix E as:

$$\alpha_3 = \frac{\frac{N_c}{N_r}\frac{R_b}{R_c}\frac{1}{V_s}\left[1+\left(\frac{N_s}{N_r}\right)^2\frac{R_b}{R_R}\right]}{\left(1+\frac{N_s}{N_r}\frac{R_b}{R_R}\right)\left[\left(\frac{N_c}{N_r}\right)^2\frac{R_b}{R_c}+\left(\frac{N_s}{N_r}\right)^2\frac{R_b}{R_R}\right]}, \qquad (15)$$

$$K_2 = \frac{R_R}{N_s}. \qquad (16)$$

18. Note that the line resistance R_s does not appear in either equation (10) or (14) indicating that the gain of the stage is independent of this resistance. Thus the quiescent power dissipated in the bridge can be limited by this resistance without affecting the gain of the stage. As pointed out below, a value of R_s too large will limit the maximum output of the stage.

19. Equations (10) and (14), the transfer functions for the bridges of figures 1(a) and 1(b) respectively, appear quite complicated. These equations are useful in an investigation of the magnitudes and types of non-linearities inherent in the circuits when "ideal components" (i.e. rectangular B-H loop cores and resistive rectifiers) are assumed. In a practical amplifier the non-linearities indicated in equations (10) and (14) are small compared to the non-linearities caused by the breakdown of the assumptions on which the equivalent circuits are based.

20. In the analysis of the reset half-cycle (see Appendices D and E) the power circuit rectifiers were assumed to have reverse voltage on them during the entire reset half-cycle. Control of the circuit is effected by increasing the volt-time integral on one reactor while decreasing it on the other. These changes in volt-time integrals are in turn effected by changing the voltages on the reactors. If the voltage on one reactor becomes high enough to overcome the supply voltage, forward current will flow through the power rectifiers associated with that reactor and form a low impedance path, shunting the control winding of that reactor and thus limiting the volt-time integral that can be applied to that reactor. For example, consider the power circuits of figures (15) and (18). As the control voltage V_c is increased in the polarity shown, the voltage e_{c_1} will increase while the voltage e_{c_2} will decrease. When the voltage $2(N_s/N_c)e_{c_1}$ tries to become greater than the supply voltage v_s the power circuit rectifiers associated with reactor 1 conduct forward current. Consequently, for these rectifiers the forward resistance R_{f_1} must be substituted for the back resistance R_R and, since $R_{f_1} << R_R$, the control circuit of reactor 1 is shunted

by a very low impedance. Thus the flux change in reactor 1 is limited at this voltage level and the gain of the bridge falls off rapidly at this point. In most practical amplifiers this effect is the primary limitation on the extent of the linear range.

21. In the analysis of the operating half-cycle (see Appendix F), the conditions for validity of the analysis are that the firing time of reactor 2, t_g be greater than zero, and the firing time of reactor 1, t_9 be less than π/ω. When either of these conditions is not satisfied the analysis of the operating half-cycle breaks down and the gain falls off rapidly. In most circuits the parameters can be adjusted so that this limit on the analysis is reached at a larger value of control voltage than the limit on the reset half-cycle discussed previously. If too large a line resistance, R_s, is used, the firing time, t_9, of reactor 1 may reach the value π/ω at a value of control voltage at which the analysis of the reset circuit still holds, thus limiting the maximum output of the amplifier.

22. Since the non-linearities indicated in equations (10) and (14) are second order effects compared to the non-linearities resulting from a breakdown of the assumptions in the analysis, they may be dropped and equation (10) can be simplified to:

$$\frac{V_L}{V_c} = \left(\frac{R_L}{R_L + R_f}\right)\left(\frac{K_1 N_c}{R_c + K_1 N_c^2}\right)\frac{N_s}{\pi}\cos^{-1}\alpha_o \,, \qquad (17)$$

and equation (14) can be simplified to:

$$\frac{V_L}{V_c} = \left(\frac{R_L}{R_L + R_f}\right)\left(\frac{K_2 N_c}{R_c + K_2 N_c^2}\right)\frac{N_s}{\pi}\cos^{-1}\alpha_o \,. \qquad (18)$$

Both of these equations have the same form:

$$\frac{V_L}{V_c} = \left(\frac{R_L}{R_L + R_f}\right)\left(\frac{K N_c}{R_c + K N_c^2}\right)\frac{N_s}{\pi}\cos^{-1}\alpha_o \,, \qquad (19)$$

where K and α_o are independent of the control turns N_c. Since the control circuit resistance R_c is determined by the control source and

the remainder of the parameters are fixed from considerations of the load and the amplifier firing angle, they are generally fixed in any application. Therefore, the control turns should be optimized for maximum gain. When the expression of equation (19) is differentiated with respect to N_c and equated to zero the condition imposed upon N_c to produce maximum gain is:

$$N_c = \sqrt{\frac{R_c}{K}} \quad . \tag{20}$$

Substitution of this expression into equation (19) yields:

$$\frac{V_L}{V_c} = \left(\frac{R_L}{R_L + R_f}\right)\sqrt{\frac{K}{R_c}}\ \frac{N_s}{2\pi}\ \cos^{-1}\alpha_o \quad . \tag{21}$$

Much good design information can be obtained from this expression; however, the results are more lucid when the power gain of the amplifier is studied. Using the expression of equation (21), the power gain, with control turns N_c adjusted according to equation (20), is:

$$\left(\frac{V_L}{V_c}\right)^2 \frac{R_c}{R_L} = \frac{R_L}{(R_L + R_f)^2}\ \frac{K N_s^2}{4\pi^2}\ \left(\cos^{-1}\alpha_o\right)^2 . \tag{22}$$

Note that this expression is independent of both control turns N_c and control circuit resistance R_c; consequently, so long as the control circuit is optimized according to equation (20) the power gain is a constant maximum independent of the impedance level of the control circuit.

23. To allow study of the effect of different parameters on the power gain, values of K_1 from equation (13) and α_o from equation (8) are substituted into equation (22) to give the power gain for the circuit with parallel reset (figure 1(a)).

$$\left(\frac{V_L}{V_c}\right)^2 \frac{R_c}{R_L} = \frac{R_L}{(R_L + R_f)^2}\left(\frac{2}{\frac{N_s^2}{R_c} + 2\frac{N_s^2}{R_R}}\right)\frac{N_s^2}{4\pi^2}\left[\cos^{-1}\frac{\frac{R_b(NI)}{N_r V_s}}{1 + \frac{N_s}{N_r}\frac{R_b}{R_R}}\right]^2 . \tag{23}$$

Substitution of α_o and K_2 from equation (16) into equation (22) yields the corresponding power gain for the bridge with series reset (figure 1(b)).

$$\left(\frac{V_L}{V_c}\right)^2 \frac{R_c}{R_L} = \frac{R_L}{(R_L + R_f)^2} \frac{R_R}{4\pi^2} \left[\cos^{-1} \frac{\frac{R_b(NI)}{N_r V_s}}{1 + \frac{N_s}{N_r}\frac{R_b}{R_R}}\right]^2. \tag{24}$$

24. Although optimization of these two expressions with respect to the various parameters is quite complicated, useful design information can be obtained by studying the expressions when ideal components are assumed.

25. First, when ideal reactors are assumed (coercive, (NI), equal to zero), the argument of the arc cos term in each of the power gain expressions goes to zero, giving for equations (23) and (24) respectively:

$$\left(\frac{V_L}{V_c}\right)^2 \frac{R_c}{R_L} = \frac{R_L}{(R_L + R_f)^2} \frac{1}{8} \frac{R_R}{2 + \left(\frac{N_1}{N_s}\right)^2 \frac{R_R}{R_b}}, \tag{25}$$

$$\left(\frac{V_L}{V_c}\right)^2 \frac{R_c}{R_L} = \frac{R_L}{(R_L + R_f)^2} \frac{R_R}{16}. \tag{26}$$

Thus with ideal reactors the gains of the bridges of figure 1 are limited principally by rectifier reverse resistance R_R.

26. When the rectifier reverse resistance is made very large the expressions of equations (23) and (24) become respectively:

$$\left(\frac{V_L}{V_c}\right)^2 \frac{R_c}{R_L} = \frac{R_L}{(R_L + R_f)^2} \frac{1}{2\pi^2} \frac{N_s^2}{N_r^2} R_b \left[\cos^{-1} \frac{R_b(NI)}{N_r V_s}\right]^2, \tag{27}$$

$$\left(\frac{V_L}{V_c}\right)^2 \frac{R_c}{R_L} = \frac{R_L}{(R_L + R_f)^2} \frac{R_R}{4\pi^2} \left[\cos^{-1} \frac{R_b(NI)}{N_r V_s}\right]^2. \tag{28}$$

27. It is evident from equation (27) that for the bridge with parallel reset the power gain is limited by the reset circuit, while in the bridge with series reset the power gain increases directly with the rectifier reverse resistance. It is pointed out that with dry-disc rectifiers the reverse resistance of a rectifier can be increased with an

attendant increase in forward resistance; consequently, since the term R_f in the above expressions contains the forward resistance of a power rectifier, caution must be used in trying to achieve higher gain by increasing the power rectifier reverse resistance. The expression of equation (28) shows that if synchronous choppers are used for the power rectifiers quite a large gain can be obtained with the bridge having series reset.

28. From the nature of the arc cosine it is evident that equation (28) can be further maximized by requiring that the reset resistance R_b be zero. This reduces equation (28) to:

$$\left(\frac{V_L}{V_c}\right)^2 \frac{R_c}{R_L} = \frac{R_L}{(R_L + R_f)^2} \cdot \frac{R_R}{16} . \qquad (29)$$

(Note that this expression is independent of the coercive, (NI).) To achieve this and still have a good linear range in the amplifier, the reset turns N_r must be greater than the power turns N_s as shown by a consideration of the firing angle (equation (8)) and a study of the equivalent circuit. One complication arises in such an adjustment. Due to the magnitudes of the voltages appearing in the reset circuit a chopping action is required to keep the reset circuit from loading the power circuit during the saturating half-cycle. This chopping action can be achieved through the use of a synchronous chopper or a biased rectifier.

CONCLUSIONS

29. The special cases for the bridges of figure 1 given above demonstrate the usefulness of this analysis. The analysis can be examined in greater detail to give more information concerning the effects of various components on the operation.

30. Since the time delay through a half-wave bridge magnetic amplifier stage is a constant, independent of gain, and since the gain is mainly determined by the power rectifier reverse resistance, "figure of merit" as applied to full-wave circuitry has no meaning in connection with the half-wave bridge. This is true because the gain is not a function of the time constant of the amplifier.

31. A conventional full-wave magnetic amplifier circuit can be broken down into two half-wave circuits; consequently, an analysis of this type is applicable to a full-wave circuit with only one generalization -- that of an additional control voltage feeding into the control circuit of each half-wave circuit from the other circuit. Such a view-point is a new approach to an analysis of full-wave circuits because most analyses in the past have started with a single-ended full-wave circuit as the fundamental building block.

APPENDIX A

ANALYSIS DURING RESET HALF-CYCLE OF CIRCUIT WITH PARALLEL RESET FOR QUIESCENT CONDITIONS ($v_c = 0$)

1. Under quiescent conditions ($v_c = 0$), the bridge of figure 1(a) is always balanced; therefore, no net induced voltage appears in the control circuit. Consequently, the control circuit can be disregarded in an analysis of quiescent conditions. Since the bridge is always balanced both reactors operate identically. Hence only one reactor need be considered.

2. At the start of the reset half-cycle ($t = 0$), both reactors are at point a in figure 5. As the line voltage builds up, the operation of the reactors proceeds from point a to point b in figure 5, reaching point b at the time t_1. In view of the assumptions concerning the reactors and rectifiers, the equivalent circuit during the time interval $0 < t < t_1$ is shown in figure 6. Additional assumptions concerning this equivalent circuit are that currents flowir during the reset half-cycle cause negligible voltage drops across the line resistance R_s and the load resistance R_L; and the circuit parameters are so adjusted that reverse voltage is always applied to the rectifiers.

3. Considering only one reactor, since both operate identically, the equivalent circuit of figure 6 is described by the following equations:

$$i_r = \frac{v_s}{R_b}, \tag{A1}$$

$$i_s = \frac{v_s}{2R_a}, \tag{A2}$$

$$2N_s i_s + N_r i_r = Ni. \tag{A3}$$

4. These equations hold for the interval of time $0 < t < t_1$, where t_1 is defined as the time at which the net ampere-turns on either reactor equals the coercive value, (NI). The time t_1 is found from the above definition and equation (A3) thus:

$$\frac{N_s}{R_a} V_s \sin \omega t_1 + \frac{N_r}{R_b} V_s \sin \omega t_1 = (NI). \tag{A4}$$

Solution of equation (A4) for the time t_1 gives:

$$t_1 = \frac{1}{\omega} \sin^{-1} \frac{\frac{R_b (NI)}{N_r V_s}}{1 + \frac{N_s}{N_r} \frac{R_b}{R_R}} . \tag{A5}$$

5. After the time t_1 the operation of the reactors proceeds from point b to point c on the loop of figure 5, arriving at point c at the time t_2. Thus, in the time interval $t_1 < t < t_2$, the equivalent circuit is that shown in figure 7. The equations describing either reactor in this equivalent circuit are:

$$v_s = i_r R_b + e_r , \tag{A6}$$

$$v_s = i_s 2R_R + \frac{2N_s}{N_r} e_r , \tag{A7}$$

$$N_r i_r + 2N_s i_s = (NI) . \tag{A8}$$

Two quantities are desired from this set of equations -- the voltage e_r to find the flux ϕ produced in the reactors during the reset half-cycle, and the time t_2 at which the voltage e_r goes to zero, such that $\pi/2\omega < t_2 < \pi/\omega$.

6. Simultaneous solution of equations (A6), (A7), and (A8) yields for the voltage e_r:

$$e_r = \frac{v_s \left[1 + \frac{N_s}{N_r} \frac{R_b}{R_R} \right] - \frac{R_b}{N_r} (NI)}{1 + 2 \left(\frac{N_s}{N_r} \right)^2 \frac{R_b}{R_R}} . \tag{A9}$$

The time t_2, defined above, is found by equating e_r to zero. The result is:

$$t_2 = \frac{\pi}{\omega} - t_1 . \tag{A10}$$

7. The flux change ϕ from figure 5 is given by Faraday's Law to be.

$$\phi = \frac{1}{N_r} \int_{t_1}^{t_2} e_r \, dt . \tag{A11}$$

Substituting equation (A9) into (A11) and evaluating the integral with the limits defined by equations (A5) and (A10) gives:

$$\phi = \frac{\frac{2V_s}{\omega N_r}\left(1+\frac{N_s}{N_r}\frac{R_b}{R_R}\right)}{1+2\left(\frac{N_s}{N_r}\right)^2\frac{R_b}{R_R}}\left[\cos\sin^{-1}\frac{\frac{R_b(NI)}{N_rV_s}}{1+\frac{N_s}{N_r}\frac{R_b}{R_R}} - \frac{\frac{R_b(NI)}{N_rV_s}}{1+\frac{N_s}{N_r}\frac{R_b}{R_R}}\cos^{-1}\frac{\frac{R_b(NI)}{N_rV_s}}{1+\frac{N_s}{N_r}\frac{R_b}{R_R}}\right]. \quad \text{(A12)}$$

To simplify the notation let:

$$\alpha_o = \frac{\frac{R_b(NI)}{N_rV_s}}{1+\frac{N_s}{N_r}\frac{R_b}{R_R}}; \quad \text{(A13)}$$

And then equation (A12) becomes:

$$\phi = \frac{\frac{2V_s}{\omega N_r}\left(1+\frac{N_s}{N_r}\frac{R_b}{R_R}\right)}{1+2\left(\frac{N_s}{N_r}\right)^2\frac{R_b}{R_R}}\left[\cos\sin^{-1}\alpha_o - \alpha_o\cos^{-1}\alpha_o\right]. \quad \text{(A14)}$$

8. During the time interval $t_2 < t < \pi/\omega$, the external circuits can not supply the coercive ampere-turns of the reactors and the reactors operate from point c to point d in figure 5. During this interval of time the equivalent circuit is once again that shown in figure 6. No flux change occurs during this interval; hence the total flux change during the reset half-cycle is given by equation (A14).

APPENDIX B

ANALYSIS DURING RESET HALF-CYCLE OF CIRCUIT WITH SERIES RESET FOR QUIESCENT CONDITIONS ($v_c = 0$)

1. Under quiescent conditions ($v_c = 0$), the bridge of figure 1(b) is always balanced. Under these conditions the net induced voltage in the control circuit is always zero; consequently, the control circuit can be disregarded in this analysis. Also, since both reactors operate identically, the operation of only one reactor need be considered.

2. At the start of the reset half-cycle ($t = 0$), both reactors are at point a in figure 5. As the line voltage increases, the operation of the reactors proceeds from point a to point b in figure 5, arriving at point b at the time t_1. Then, for the interval of time $0 < t < t_1$, the equivalent circuit of figure 1(b) is shown in figure 8, assuming once again that currents flowing during the reset half-cycle cause negligible voltage drops across the line resistance R_s and the load resistance R_L, and the parameters are adjusted to maintain reverse voltage on the rectifiers.

3. Considering only one reactor, the circuit of figure 8 is described by the following equations:

$$i_r = \frac{v_s}{R_b}, \tag{B1}$$

$$i_s = \frac{v_s}{2R_R}, \tag{B2}$$

$$2N_s i_s + N_r i_r = Ni. \tag{B3}$$

These equations hold for the interval of time $0 < t < t_1$ where t_1 is defined as the time at which the net ampere-turns on either reactor reaches the coercive value, (NI). At time t_1 equations (B1) and (B2) substituted into equation (B3) yield:

$$\frac{N_s}{R_R} V_s \sin \omega t_1 + \frac{N_r}{R_b} V_s \sin \omega t_1 = (NI). \tag{B4}$$

Solution of equation (B4) for the time t_1 gives:

$$t_1 = \frac{1}{\omega} \sin^{-1} \frac{\frac{R_b(NI)}{N_r V_s}}{1 + \frac{N_s}{N_r}\frac{R_b}{R_R}} . \qquad (B5)$$

4. After the time t_1 the operation of the reactors proceeds from point b to point c on the loop of figure 5, arriving at point c at the time t_2. In the time interval $t_1 < t < t_2$ the equivalent circuit is shown in figure 9. The equations describing this circuit are:

$$V_s = 2e_r + i_r R_b , \qquad (B6)$$

$$V_s = 2\frac{N_s}{N_r} e_r + i_s 2R_R , \qquad (B7)$$

$$2N_s i_s + N_r i_r = (NI)_c . \qquad (B8)$$

Two quantities are desired from this set of equations -- the voltage e_r to allow calculation of the flux ϕ that is changed in the reactors during the reset half-cycle, and the time t_2 at which the voltage e_r goes to zero such that $\pi/2\omega < t_2 < \pi/\omega$.

5. Simultaneous solution of equations (B6), (B7) and (B8) yields for the voltage e_r:

$$e_r = \frac{V_s\left[1 + \frac{N_s}{N_r}\frac{R_b}{R_R}\right] - \frac{R_b(NI)}{N_r}}{2\left[1 + \left(\frac{N_s}{N_r}\right)^2 \frac{R_b}{R_R}\right]} . \qquad (B9)$$

The time t_2, defined above, is found by equating the voltage e_r to zero and is found to be:

$$t_2 = \frac{\pi}{\omega} - t_1 . \qquad (B10)$$

6. The flux change ϕ (see figure 5) is found by Faraday's Law:

$$\phi = \frac{1}{N_r}\int_{t_1}^{t_2} e_r \, dt . \qquad (B11)$$

Substitution of equation (B9) into (B11) and evaluation of the integral with the limits defined by equations (B5) and (B10) leads to the result:

$$\phi = \frac{\frac{V_s}{\omega N_r}\left(1+\frac{N_s}{N_r}\frac{R_b}{R_R}\right)}{1+\left(\frac{N_s}{N_r}\right)^2\frac{R_b}{R_R}}\left[\cos\sin^{-1}\frac{\frac{R_b(NI)}{N_r V_s}}{1+\frac{N_s}{N_r}\frac{R_b}{R_R}} - \frac{\frac{R_b(NI)}{N_r V_s}}{1+\frac{N_s}{N_r}\frac{R_b}{R_R}}\cos^{-1}\frac{\frac{R_b(NI)}{N_r V_s}}{1+\frac{N_s}{N_r}\frac{R_b}{R_R}}\right]. \quad (B12)$$

With the definition,

$$\alpha_o = \frac{\frac{R_b(NI)}{N_r V_s}}{1+\frac{N_s}{N_r}\frac{R_b}{R_R}}, \quad (B13)$$

equation (B12) becomes:

$$\phi = \frac{\frac{V_s}{\omega N_r}\left(1+\frac{N_s}{N_r}\frac{R_b}{R_R}\right)}{1+\left(\frac{N_s}{N_r}\right)^2\frac{R_b}{R_R}}\left[\cos\sin^{-1}\alpha_o - \alpha_o\cos^{-1}\alpha_o\right]. \quad (B14)$$

7. During the time interval $t_2 < t < \pi/\omega$ the reactors operate from point c to point d in figure 5 and the equivalent circuit is once again that shown in figure 8. No flux change occurs during this interval; therefore, the total flux change during the reset half-cycle is given by equation (B14).

APPENDIX C

ANALYSIS DURING OPERATING HALF-CYCLE OF BOTH CIRCUITS FOR QUIESCENT CONDITIONS ($v_c = 0$)

1. With the assumption that the reset circuits cause negligible loading on the reactors during the operating half-cycle, the equivalent circuits of figures 1(a) and 1(b) become the same for this period of operation. At the start of the operating half-cycle both reactors are at point d of figure 5. The currents that flow while the cores are unsaturated are assumed to cause negligible voltage drops across the line resistance R_s, the rectifier forward resistance R_f, and the load resistance R_L; therefore, the operation of the cores changes from point d to point e in figure 5 in essentially zero time. This leads to the equivalent circuit of figure 10 for the time interval $0 < t < t_3$ where t_3 is the time at which the operation of the reactors reaches point f in figure 5.

2. The net induced voltage in the control circuit is zero; therefore, the control circuit is omitted from the equivalent circuit.

3. In view of the assumptions, the supply voltage v_s is applied directly across the power windings as shown in the equivalent circuit; consequently, the time t_3 is found from Faraday's Law:

$$\phi = \frac{1}{2N_s}\int_0^{t_3} v_s\, dt, \qquad (C1)$$

where ϕ is the flux level in the two reactors after the next previous reset half-cycle as shown on the loop of figure 5. Evaluating the integral in equation (C1) leads to:

$$\cos \omega t_3 = 1 - \frac{2\omega N_s \phi}{V_s}. \qquad (C2)$$

Equation (C2) gives the quiescent "firing angle" ωt_3 as a function of the flux ϕ produced during the next previous reset half-cycle and the system parameters.

4. During the time interval $t_3 < t < \pi/\omega$ the reactors are saturated and operate at the saturation flux level ϕ_s (see figure 5). During this time interval the equivalent circuit is that shown in figure 11. Note that the bridge is still balanced; therefore, no current flows through the load resistance R_L during this interval. The current flowing in the bridge during this interval is:

$$2 i_s = \frac{V_s}{R_s + R_f} , \tag{C3}$$

where i_s is the current flowing in each arm of the bridge.

5. During the time interval $t_3 < t < \pi/\omega$ the instantaneous power into the bridge is

$$p = 2 i_s V_s , \tag{C4}$$

and the average quiescent power is given by:

$$P_q = \frac{\omega}{2\pi} \int_{t_3}^{\frac{\pi}{\omega}} 2 i_s V_s \, dt. \tag{C5}$$

Substitution of equation (C3) into equation (C5) and evaluation of the integral gives the quiescent power:

$$P_q = \frac{1}{2\pi} \frac{V_s^2}{(R_s + R_f)} \left[\pi - \omega t_3 + \sin \omega t_3 \cos \omega t_3\right], \tag{C6}$$

If the quiescent power P_q is desired in terms of the "firing angle" ωt_3, equation (C6) is used. Substitution of equation (C2) into (C6) leads to:

$$P_q = \frac{1}{2\pi} \frac{V_s^2}{(R_s + R_f)} \left[\pi - \cos^{-1}\left(1 - \frac{2\omega N_s \phi}{V_s}\right) + \left(1 - \frac{2\omega N_s \phi}{V_s}\right) \sin \cos^{-1}\left(1 - \frac{2\omega N_s \phi}{V_s}\right)\right]. \tag{C7}$$

When the quiescent power is desired as a function of system parameters only, the value of the flux ϕ for the parallel reset circuit can be substituted from equation (A14) of Appendix A and for the series reset circuit from equation (B14) of Appendix B. In this manner the quiescent power is determined for either bridge circuit of figure 1 as a function of adjustable system parameters.

6. If the average value of the quiescent current in each arm of the bridge is desired, it can be found from equation (C3):

$$I_s = \frac{\omega}{2\pi} \int_{t_3}^{\frac{\pi}{\omega}} \frac{V_s}{2(R_s + R_f)}\, dt. \qquad (C8)$$

Evaluation of the integral gives:

$$I_s = \frac{V_s}{4\pi (R_s + R_f)} (1 + \cos \omega t_3). \qquad (C9)$$

And substituting from equation (C2), (C9) becomes:

$$I_s = \frac{V_s}{2\pi (R_s + R_f)} \left(1 - \frac{\omega N_s \phi}{V_s}\right). \qquad (C10)$$

The appropriate value for the flux ϕ can be substituted into this expression to obtain the average value of the quiescent current as a function of adjustable system parameters.

7. Another quantity that may be desired from an analysis of the quiescent conditions is the firing angle ωt_3 as a function of the system parameters. For the bridge with parallel reset of figure 1(a) this function is found by substitution of equation (A14) from Appendix A into equation (C2) to give

$$\cos \omega t_3 = 1 - \frac{4 \frac{N_s}{N_r}\left(1 + \frac{N_s}{N_r} \frac{R_b}{R_R}\right)}{1 + 2\left(\frac{N_s}{N_r}\right)^2 \frac{R_b}{R_R}} \left[\cos \sin^{-1}\alpha_o - \alpha_o \cos^{-1}\alpha_o\right], \qquad (C11)$$

where α_o is defined by equation (A13) of Appendix A. The firing angle ωt_3 for the bridge with series reset of figure 1(b) is found as a function of the system parameters by substituting equation (B14) from Appendix B into equation (C2), thus:

$$\cos \omega t_3 = 1 - \frac{2\frac{N_s}{N_r}\left(1+\frac{N_s}{N_r}\frac{R_b}{R_R}\right)}{1+\left(\frac{N_s}{N_r}\right)^2\frac{R_b}{R_R}}\left[\cos \sin^{-1}\alpha_o - \alpha_o \cos^{-1}\alpha_o\right], \qquad (C12)$$

where α_o is defined as above.

APPENDIX D

ANALYSIS DURING RESET HALF-CYCLE OF CIRCUIT WITH PARALLEL RESET FOR DIRECT CONTROL VOLTAGE, V_c

1. During the reset half-cycle, the control voltage V_c causes a flux difference $\Delta\phi$ between the two reactors. This flux difference $\Delta\phi$ in turn determines the amount of load current that flows on the next operating half-cycle. Therefore, the quantity to be found from an analysis of the reset half-cycle is the flux difference $\Delta\phi$ as a function of the control voltage V_c.

2. When the control voltage has the polarity shown in figure 1(a) and $t = 0$ (start of the reset half-cycle), reactor 1 is operating at point a and reactor 2 is at point b on the loop of figure 12. The distance ac is equal to the distance bc. As the supply voltage increases, the operation of both reactors will proceed to the left as shown by the arrows in figure 12, with reactor 1 reaching point d at the time t_4. The operation of reactor 2 will reach point d at a later time, t_5.

3. During the time interval $0 < t < t_4$ the equivalent circuit of figure 1(a) is given in figure 13. Some assumptions are made concerning this circuit. Currents that flow during the reset half-cycle cause negligible voltage drops across the load resistance, R_L, and the line resistance, R_s. The total reset circuit resistance including rectifier and winding resistance is lumped into the resistance R_b. Also, the parameters must be adjusted so that reverse voltage is on the power circuit rectifiers. (In practical cases, this is the assumption that breaks down under very large signal conditions and limits the maximum output of the stage.) The equations describing the equivalent circuit of figure 13 are:

$$i_{r_1} = i_{r_2} = \frac{V_c}{R_b}, \tag{D1}$$

$$i_{s_1} = i_{s_2} = \frac{V_c}{2R_R}, \tag{D2}$$

$$i_c = \frac{V_c}{R_c}. \tag{D3}$$

Since both reactors are in a saturated condition during this interval no flux charge will occur in either reactor. The time t_4 is defined as the time at which the operation of reactor 1 reaches point d

in figure 12. This means that time t_4 is the time at which the net ampere-turns on reactor 1 equal the coercive value (NI):

$$N_r i_{r_1}(t_4) + 2N_s i_{s_1}(t_4) + N_c i_c(t_4) = (NI). \tag{D4}$$

Substituting equations (D1), (D2), and (D3) with the definition of V_s given in figure 13 leads to:

$$\frac{N_r}{R_b} V_s \sin \omega t_4 + \frac{N_s}{R_R} V_s \sin \omega t_4 + \frac{N_c}{R_c} V_c = (NI). \tag{D5}$$

Solution of equation (D5) for the time t_4 gives:

$$t_4 = \frac{1}{\omega} \sin^{-1} \left[\frac{\frac{R_b(NI)}{N_r V_s} - \frac{N_c}{N_r} \frac{R_b}{R_c} \frac{V_c}{V_s}}{1 + \frac{N_s}{N_r} \frac{R_b}{R_R}} \right]. \tag{D6}$$

If, as in equation (A13) of Appendix A, a factor α_o is defined as

$$\alpha_o = \frac{\frac{R_b(NI)}{N_r V_s}}{1 + \frac{N_s}{N_r} \frac{R_b}{R_R}}, \tag{D7}$$

and another factor α_1 is defined as

$$\alpha_1 = \frac{\frac{N_c}{N_r} \frac{R_b}{R_c} \frac{1}{V_s}}{1 + \frac{N_s}{N_r} \frac{R_b}{R_R}}, \tag{D8}$$

Then equation (D6) becomes

$$t_4 = \frac{1}{\omega} \sin^{-1} (\alpha_o - \alpha_1 V_c). \tag{D9}$$

4. After the time t_4 the operation of reactor 1 proceeds down the side of the loop as shown by the arrows in figure 12, while the operation of reactor 2 continues along the top of the loop arriving at point d at time t_5. During the interval $t_4 < t < t_5$ an amount of flux $\Delta \phi_1$ is changed in reactor 1 while no flux is changed in reactor 2. During this interval the equivalent circuit is shown in figure 14 with the previous assumptions still applying. The equations describing this circuit are:

$$v_s = \frac{N_r}{N_c} e_{c_1} + i_{r_1} R_b \,, \tag{D10}$$

$$v_s = \frac{2N_s}{N_c} e_{c_1} + i_{s_1} 2R_R \,, \tag{D11}$$

$$V_c = e_{c_1} + i_c R_c \,, \tag{D12}$$

$$2N_s i_{s_1} + N_r i_{r_1} + N_c i_c = (NI) \,, \tag{D13}$$

$$i_{s_2} = \frac{v_s}{2R_R} \,, \tag{D14}$$

$$i_{r_2} = \frac{v_s}{R_b} \,. \tag{D15}$$

Two quantities are desired from this set of equations -- the voltage e_{c_1} to allow calculation of the flux change $\Delta \phi_1$ occurring in reactor 1 during this interval, and the time t_5 at which the net ampere-turns in reactor 2 equals the coercive value (NI).

5. The voltage e_{c_1} on the control winding of reactor 1 during the interval $t_4 < t < t_5$ is found by simultaneous solution of equations (D10) through (D13) to be:

$$e_{c_1} = \frac{\frac{N_s}{N_r}\left[1 + \frac{N_s}{N_r}\frac{R_b}{R_R}\right]}{1 + \left(\frac{N_c}{N_r}\right)^2 \frac{R_b}{R_c} + 2\left(\frac{N_s}{N_r}\right)^2 \frac{R_b}{R_R}} V_s \sin \omega t + \frac{\left(\frac{N_c}{N_r}\right)^2 \frac{R_b}{R_c} V_c - \frac{N_s}{N_r}\frac{R_b}{N_r}(NI)}{1 + \left(\frac{N_s}{N_r}\right)^2 \frac{R_b}{R_c} + 2\left(\frac{N_s}{N_r}\right)^2 \frac{R_b}{R_R}} \,. \tag{D16}$$

The time t_5 is found by equating the net ampere turns on reactor 2 to the coercive value thus:

$$2N_s i_{s_2}(t_5) + N_r i_{r_2}(t_5) - N_c i_c(t_5) = (NI). \tag{D17}$$

Substitution of the appropriate values of the currents from equations (D12), (D14), and (D15) leads to the evaluation of the time t_5:

$$t_5 = \frac{1}{\omega} \sin^{-1} \left\{ \frac{\frac{R_b(NI)}{N_r V_s}}{1 + \frac{N_s}{N_r}\frac{R_b}{R_R}} + \frac{\frac{N_c}{N_r}\frac{R_b}{R_c}\frac{V_c}{V_s}\left[1 + 2\left(\frac{N_s}{N_r}\right)^2 \frac{R_b}{R_R}\right]}{\left(1 + \frac{N_s}{N_r}\frac{R_b}{R_R}\right)\left[1 + 2\left(\frac{N_s}{N_r}\right)^2 \frac{R_b}{R_c} + 2\left(\frac{N_s}{N_r}\right)^2 \frac{R_b}{R_R}\right]} \right\}. \tag{D18}$$

Using the value of α_o defined in equation (D10) with the definition of α_2:

$$\alpha_2 = \frac{\frac{N_c}{N_r}\frac{R_b}{R_c}\frac{1}{V_s}\left[1 + 2\left(\frac{N_s}{N_r}\right)^2 \frac{R_b}{R_R}\right]}{\left(1 + \frac{N_s}{N_r}\frac{R_b}{R_R}\right)\left[1 + 2\left(\frac{N_s}{N_r}\right)^2 \frac{R_b}{R_c} + 2\left(\frac{N_s}{N_r}\right)^2 \frac{R_b}{R_R}\right]}, \tag{D19}$$

equation (D18) becomes:

$$t_5 = \frac{1}{\omega} \sin^{-1}(\alpha_o + \alpha_2 V_c). \tag{D20}$$

6. During the interval of time $t_4 < t < t_5$ no flux change occurs in reactor 2; therefore, any flux change that occurs in reactor 1 during this interval will contribute to the total differential flux $\Delta\phi$ between the reactors at the end of the reset half-cycle. Denoting the flux change in reactor 1 during the interval $t_4 < t < t_5$ as $\Delta\phi_1$, it is found by Faraday's Law:

$$\Delta\phi_1 = \frac{1}{N_c}\int_{t_4}^{t_5} e_{c_1}\,dt. \tag{D21}$$

Substituting equation (D16) into equation (D21) and performing the integration leads to:

$$\Delta\phi_1 = \frac{1}{N_c}\left[\frac{\frac{N_c}{N_r}\left(1+\frac{N_s}{N_r}\frac{R_b}{R_R}\right)}{1+\left(\frac{N_c}{N_r}\right)^2\frac{R_b}{R_c}+2\left(\frac{N_s}{N_r}\right)^2\frac{R_b}{R_R}}\frac{V_s}{\omega}\left(\cos\omega t_4-\cos\omega t_5\right)\right.$$

$$\left.+\frac{\left(\frac{N_c}{N_r}\right)^2\frac{R_b}{R_c}V_c-\frac{N_c}{N_r}\frac{R_b}{N_r}(NI)}{1+\left(\frac{N_c}{N_r}\right)^2\frac{R_b}{R_c}+2\left(\frac{N_s}{N_r}\right)^2\frac{R_b}{R_R}}\left(t_5-t_4\right)\right]. \tag{D22}$$

Substituting into equation (D22) from equations (D9) for t_4, (D20) for t_5, (D7) for α_0, and the definition

$$\beta_1 = 1+\left(\frac{N_c}{N_r}\right)^2\frac{R_b}{R_c}+2\left(\frac{N_s}{N_r}\right)^2\frac{R_b}{R_R}, \tag{D23}$$

and simplification of the resulting expression yields:

$$\Delta\phi_1 = \frac{V_s}{\omega N_r}\frac{\left(1+\frac{N_s}{N_r}\frac{R_b}{R_R}\right)}{\beta_1}\left\{\cos\sin^{-1}(\alpha_0-\alpha_1 V_c)-\cos\sin^{-1}(\alpha_0+\alpha_2 V_c)\right.$$

$$\left.+\left(\frac{\frac{N_c}{N_r}\frac{R_b}{R_c}\frac{V_c}{V_s}}{1+\frac{N_s}{N_r}\frac{R_b}{R_R}}-\alpha_0\right)\left[\sin^{-1}(\alpha_0+\alpha_2 V_c)-\sin^{-1}(\alpha_0-\alpha_1 V_c)\right]\right\}. \tag{D24}$$

7. At the time t_5 reactor 2 reaches point d of figure 12 and remains unsaturated (net ampere-turns equal to the coercive value $(\overline{NI})$) until time t_6 when the operation of reactor 2 reaches point e on the loop of figure 12. During this interval of time $(t_5 < t < t_6)$ the equivalent circuit is that shown in figure 15. (The previous assumptions still hold.) The equations describing this equivalent circuit are:

$$v_s = \frac{N_r}{N_c} e_{c_1} + i_{r_1} R_b \,, \tag{D25}$$

$$v_s = \frac{2N_s}{N_c} e_{c_1} + i_{s_1} 2R_R \,, \tag{D26}$$

$$v_s = \frac{N_r}{N_c} e_{c_2} + i_{r_2} R_b \,, \tag{D27}$$

$$v_s = \frac{2N_s}{N_c} e_{c_2} + i_{s_2} 2R_R \,, \tag{D28}$$

$$V_c = e_{c_1} - e_{c_2} + i_c R_c \,, \tag{D29}$$

$$2N_s i_{s_1} + N_r i_{r_1} + N_c i_c = (NI) \,, \tag{D30}$$

$$2N_s i_{s_2} + N_r i_{r_2} - N_c i_c = (NI) \,. \tag{D31}$$

Two quantities are desired from this set of equations -- the voltage $(e_{c_1} - e_{c_2})$ to be used in calculating the flux difference $\Delta\phi_2$ established between reactors 1 and 2 during this interval; and the time t_6 which is defined as the time at which the voltage e_{c_2} goes to zero such that $\pi/2\omega < t_6 < \pi/\omega$.

8. Simultaneous solution of equations (D25) through (D31) for the voltage $(e_{c_1} - e_{c_2})$ yields

$$e_{c_1} - e_{c_2} = \frac{2\left(\frac{N_s}{N_r}\right)^2 \frac{R_b}{R_c} V_c}{1 + 2\left(\frac{N_s}{N_r}\right)^2 \frac{R_b}{R_c} + 2\left(\frac{N_s}{N_r}\right)^2 \frac{R_b}{R_R}} \,. \tag{D32}$$

Note that this equation can be simplified to

$$e_{c_1} - e_{c_2} = \frac{K_1 N_c^2}{R_c + K_1 N_c^2} V_c \,, \tag{D33}$$

Where

$$K_1 = \frac{2}{\frac{N_b^2}{R_b} + 2\frac{N_s^2}{R_R}} \,. \tag{D34}$$

The time t_6 can be found by solving equations (D25) through (D31) for the voltage e_{c_2} and finding the time such that $\pi/2\omega < t_6 < \pi/\omega$, that makes this voltage zero. Such a process yields for the time t_6:

$$t_6 = \frac{\pi}{\omega} - t_5 \,. \tag{D35}$$

9. The flux difference $\Delta \phi_2$ produced between the levels in reactors 1 and 2 during the time interval $t_5 < t < t_6$ is found from Faraday's Law:

$$\Delta \phi_2 = \frac{1}{N_c} \int_{t_5}^{t_6} (e_{c_1} - e_{c_2})\, dt. \tag{D36}$$

Substitution of the voltage $(e_{c_1} - e_{c_2})$ from equation (D33) into this expression and evaluation of the integral yields:

$$\Delta \phi_2 = \frac{K_1 N_c}{R_c + K_1 N_c^2} V_c \left(\frac{\pi}{\omega} - 2t_5\right). \tag{D37}$$

Substituting from equation (D20) for time t_5 and making use of the identity:

$$\cos^{-1} a = \frac{\pi}{2} - \sin^{-1} a \,, \tag{D38}$$

equation (D37) becomes:

$$\Delta \phi_2 = \frac{2}{\omega} \frac{K_1 N_c}{R_c + K_1 N_c^2} V_c \cos^{-1}(\alpha_0 + \alpha_2 V_c). \tag{D39}$$

10. After the time t_6 the operation of reactor 1 continues down the side of the loop toward point f in figure 12, while the operation of reactor 2 goes from point e toward point g in the same figure. Defining

the time t_7 as the time at which reactor 1 reaches point f of figure 12, the equivalent circuit for the time interval $t_6 < t < t_7$ is once again that shown in figure 14 described by equations (D10) through (D15). During this time interval no flux is changed in reactor 2, but an amount of flux is changed in reactor 1 and solution of equations (D10) through (D15) will show that this flux change is the same as $\Delta \phi_1$ (see equation (D24) while the time t_7 is:

$$t_7 = \frac{\pi}{\omega} - t_4 \; , \qquad \text{(D40)}$$

where time t_4 is given by equation (D9).

11. During the time interval $t_7 < t < \pi/\omega$ no flux is changed in either reactor; consequently the net differential flux $\Delta\phi$ produced between the flux levels in reactors 1 and 2 due to the control voltage V_c during the reset half-cycle is:

$$\Delta\phi = 2\Delta\phi_1 + \Delta\phi_2 \; , \qquad \text{(D41)}$$

where $\Delta \phi_1$ is given by equation (D24) and $\Delta \phi_2$ by equation (D39). Substitution of these values into equation (D41) yields:

$$\Delta\phi = \frac{K_1 N_c}{R_c + K_1 N_c^2} \frac{2V_c}{\omega} \cos^{-1}(\alpha_0 + \alpha_2 V_c)$$

$$+ \frac{V_s}{\omega N_r} \frac{\left(1 + \frac{N_s}{N_r}\frac{R_b}{R_R}\right)}{\beta_1} \left\{ \cos \sin^{-1}(\alpha_0 - \alpha_1 V_c) - \cos \sin^{-1}(\alpha_0 + \alpha_2 V_c) \right.$$

$$\left. + \left(\frac{\frac{N_s}{N_r}\frac{R_b}{R_c}\frac{V_c}{V_s}}{1 + \frac{N_s}{N_r}\frac{R_b}{R_R}} - \alpha_0 \right) \left[\sin^{-1}(\alpha_0 + \alpha_2 V_c) - \sin^{-1}(\alpha_0 - \alpha_1 V_c) \right] \right\} . \qquad \text{(D42)}$$

Note that for small signals ($V_c \rightarrow 0$) equation (D42) reduces to:

$$\Delta\phi = \frac{K_1 N_c}{R_c + K_1 N_c^2} \frac{2V_c}{\omega} \cos^{-1}\alpha_o . \qquad (D43)$$

Which demonstrates that for small signals the flux difference $\Delta\phi$ is a linear function of the control voltage.

APPENDIX E

ANALYSIS DURING RESET HALF-CYCLE OF CIRCUIT WITH SERIES RESET FOR DIRECT CONTROL VOLTAGE, V_c

1. When the control voltage has the polarity shown in figure 1(b) and t = 0 (start of the reset half-cycle), reactor 1 is operating at point a and reactor 2 is at point b on the loop of figure 12. As the supply voltage increases, the operation of both reactors proceeds to the left as shown by the arrows in figure 12, with reactor 1 reaching point d at time t_4. The operation of reactor 2 will reach point d at a later time t_5.

2. Some assumptions are made to simplify the equivalent circuits during the reset half-cycle. Currents flowing during the reset half-cycle are sufficiently small that negligible voltage drops occur across the line resistance R_s and the load resistance R_L. All the reset circuit resistance (rectifier forward and winding) is lumped into R_b. The circuit parameters must be adjusted to maintain reverse voltage on the power circuit rectifiers. If this is not satisfied the control circuit will be loaded by the low rectifier forward resistance reflected through the power windings and very little control can be exercised. This is the condition that normally limits the maximum output of the amplifier.

3. In view of these assumptions the equivalent circuit of figure 1(b) for the interval of time $0 < t < t_4$ is given in figure 16. The equations describing this circuit are:

$$i_r = \frac{v_s}{R_b}, \tag{E1}$$

$$i_{s_1} = i_{s_2} = \frac{v_s}{2R_s}, \tag{E2}$$

$$i_c = \frac{V_s}{R_c}. \tag{E3}$$

The operation of reactor 1 will reach point d at time t_4 which is defined as the time at which the net ampere-turns on reactor 1 are equal to the coercive value (NI):

$$N_r i_r(t_4) + 2N_s i_{s_1}(t_4) + N_c i_c(t_4) = (NI). \tag{E4}$$

Substituting into equation (E4) from (E1), (E2) and (E3) with the value for the supply voltage given in figure 16 yields:

$$\frac{N_r}{R_b} V_s \sin \omega t_4 + \frac{N_s}{R_a} V_s \sin \omega t_4 + \frac{N_c}{R_c} V_c = (NI). \tag{E5}$$

Solution of this expression for the time t_4 gives:

$$t_4 = \frac{1}{\omega} \sin^{-1} \left[\frac{\frac{R_b (NI)}{i_r V_s} - \frac{N_c}{N_r} \frac{R_b}{R_c} \frac{V_c}{V_s}}{1 + \frac{N_s}{N_r} \frac{R_b}{R_a}} \right]. \tag{E6}$$

Using the definitions of α_0 and α_1 as given in Appendix D:

$$\alpha_0 = \frac{\frac{R_b (NI)}{N_r V_s}}{1 + \frac{N_s}{N_r} \frac{R_b}{R_a}}, \tag{E7}$$

and

$$\alpha_1 = \frac{\frac{N_c}{N_r} \frac{R_b}{R_c} \frac{1}{V_s}}{1 + \frac{N_s}{N_r} \frac{R_b}{R_a}}, \tag{E8}$$

Equation (E6) becomes:

$$t_4 = \frac{1}{\omega} \sin^{-1} (\alpha_0 - \alpha_1 V_c). \tag{E9}$$

4. After the time t_4 the operation of reactor 1 proceeds down the side of the loop as shown by the arrows in figure 12, while the operation of reactor 2 continues along the top of the loop arriving at point d at time t_5. During the interval $t_4 < t < t_5$ no flux is changed in reactor 2, but a flux change $\Delta \phi_1$ occurs in reactor 1. During this interval the equivalent circuit is shown in figure 17. The equations describing this circuit are:

$$v_s = \frac{N_r}{N_c} e_{c_1} + i_r R_b, \tag{E10}$$

$$V_s = \frac{2N_s}{N_c} e_{c_1} + i_{s_1} 2R_R , \tag{E11}$$

$$V_c = e_{c_1} + i_c R_c , \tag{E12}$$

$$2N_s i_{s_1} + N_r i_r + N_c i_c = (NI) , \tag{E13}$$

$$i_{s_2} = \frac{V_s}{2R_R} . \tag{E14}$$

Two quantities are desired from these equations -- the voltage e_{c_1} to allow calculation of $\Delta \phi_1$, and the time t_5 at which the operation of reactor 2 reaches point d on the loop of figure 12.

5. The voltage e_{c_1} on the control winding of reactor 1 during the interval $t_4 < t < t_5$ is found by solving equations (E10) through (E14) to be:

$$e_{c_1} = \frac{\frac{N_c}{N_r}\left(1 + \frac{N_s}{N_r}\frac{R_b}{R_R}\right)}{1 + \left(\frac{N_s}{N_r}\right)^2 \frac{R_b}{R_c} + 2\left(\frac{N_s}{N_r}\right)^2 \frac{R_b}{R_R}} V_s \sin \omega t + \frac{\left(\frac{N_s}{N_r}\right)^2 \frac{R_b}{R_c} V_c - \frac{N_c}{N_r}\frac{R_b (NI)}{N_r}}{1 + \left(\frac{N_c}{N_r}\right)^2 \frac{R_b}{R_c} + 2\left(\frac{N_s}{N_r}\right)^2 \frac{R_b}{R_R}} . \tag{E15}$$

The time t_5 is found by equating the net ampere-turns on reactor 2 to the coercive value:

$$2N_s i_{s_2}(t_5) + N_r i_r(t_5) - N_c i_c(t_5) = (NI) . \tag{E16}$$

Substitution of the appropriate values of currents from equations (E10), (E12), and (E14) leads to the evaluation of t_5:

$$t_5 = \frac{1}{\omega} \sin^{-1} \left\{ \frac{\frac{R_b (NI)}{N_r V_s}}{1 + \frac{N_s}{N_r}\frac{R_b}{R_R}} + \frac{\frac{N_c}{N_r}\frac{R_b}{R_c}\frac{V_c}{V_s}\left[1 + \left(\frac{N_s}{N_r}\right)^2 \frac{R_b}{R_R}\right]}{\left(1 + \frac{N_s}{N_r}\frac{R_b}{R_R}\right)\left[\left(\frac{N_c}{N_r}\right)^2 \frac{R_b}{R_c} + \left(\frac{N_c}{N_r}\right)^2 \frac{R_b}{R_R}\right]} \right\} . \tag{E17}$$

Using the definition of α_o from equation (E7) and the definition

$$\alpha_3 = \frac{\frac{N_s}{N_r}\frac{R_b}{R_c}\frac{1}{\tau_s}\left[1+\left(\frac{N_s}{N_r}\right)^2\frac{R_b}{R_R}\right]}{\left(1+\frac{N_s}{N_r}\frac{R_b}{R_R}\right)\left[\left(\frac{N_c}{N_r}\right)^2\frac{R_b}{R_c}+\left(\frac{N_s}{N_r}\right)^2\frac{R_b}{R_R}\right]}, \tag{E18}$$

Equation (E17) becomes

$$t_5 = \frac{1}{\omega}\sin^{-1}\left(\alpha_0 + \alpha_3 V_c\right). \tag{E19}$$

6. During the interval of time $t_4 < t < t_5$ no flux change occurs in reactor 2; consequently, the flux change $\Delta\phi_1$ which occurs in reactor 1 during this interval contributes directly to the net differential flux produced between the reactors during the reset half-cycle. The flux difference $\Delta\phi_1$ can be found from Faraday's Law:

$$\Delta\phi_1 = \frac{1}{N_c}\int_{t_4}^{t_5} e_{c_1}\,dt. \tag{E20}$$

Substituting equation (E15) into (E20) and performing the integration yields:

$$\Delta\phi_1 = \frac{1}{N_c}\left\{\frac{\frac{N_c}{N_r}\left(1+\frac{N_s}{N_r}\frac{R_b}{R_R}\right)}{1+\left(\frac{N_s}{N_r}\right)^2\frac{R_b}{R_c}+2\left(\frac{N_s}{N_r}\right)^2\frac{R_b}{R_R}}\frac{V_s}{\omega}\left(\cos\omega t_4 - \cos\omega t_5\right)\right.$$

$$\left. + \frac{\left(\frac{N_c}{N_r}\right)^2\frac{R_b}{R_c}V_c - \frac{N_c}{N_r}\frac{R_b(NI)}{N_r}}{1+\left(\frac{N_s}{N_r}\right)^2\frac{R_b}{R_c}+2\left(\frac{N_s}{N_r}\right)^2\frac{R_b}{R_R}}\left(t_5 - t_4\right)\right\}. \tag{E21}$$

Using the definitions of t_4 from equation (E9) and t_5 from (E19) and β_1 from equation (D23) of Appendix D, equation (E21) becomes:

$$\Delta\phi_1 = \frac{V_s}{\omega N_r}\,\frac{\left(1+\frac{N_s}{N_r}\frac{R_b}{R_R}\right)}{\beta_1}\Bigg\{\cos\sin^{-1}(\alpha_0-\alpha_1 V_c)-\cos\sin^{-1}(\alpha_0+\alpha_2 V_c)$$

$$+\left(\frac{\frac{N_c}{N_r}\frac{R_b}{R_c}\frac{V_c}{V_s}}{1+\frac{N_s}{N_r}\frac{R_b}{R_R}}-\alpha_0\right)\left[\sin^{-1}(\alpha_0+\alpha_2 V_c)-\sin^{-1}(\alpha_0-\alpha_1 V_c)\right]\Bigg\}. \qquad (E22)$$

7. At the time t_5, reactor 2 reaches point d of figure 12 and remains unsaturated until time t_6 when the operation of reactor 2 reaches point e on the loop of figure 12. During this interval of time ($t_5 < t < t_6$) the equivalent circuit is that shown in figure 18. The equations describing this circuit are:

$$V_s = \frac{N_r}{N_c}e_{c_1} + \frac{N_r}{N_c}e_{c_2} + i_r R_b, \qquad (E23)$$

$$V_s = \frac{2N_s}{N_c}e_{c_1} + i_{s_1}2R_R, \qquad (E24)$$

$$V_s = \frac{2N_s}{N_c}e_{c_2} + i_{s_2}2R_R, \qquad (E25)$$

$$V_c = e_{c_1} - e_{c_2} + i_c R_c, \qquad (E26)$$

$$N_r i_r + 2N_s i_{s_1} + N_c i_c = (NI), \qquad (E27)$$

$$N_r i_r + 2N_s i_{s_2} - N_c i_c = (NI). \qquad (E28)$$

Two quantities are desired from this set of equations -- the voltage $(e_{c_1} - e_{c_2})$ to be used in calculating the flux difference $\Delta\phi_2$ established between the reactors during this interval, and the time t_6 at which the voltage e_{c_2} goes to zero such that $\pi/2\omega < t_6 < \pi/\omega$.

8. Solution of equations (E23) through (E28) for the voltage $(e_{c_1} - e_{c_2})$ yields:

$$e_{c_1} - e_{c_2} = \frac{\frac{N_c^2}{N_s^2}R_R V_c}{R_c + \frac{N_c^2}{N_s^2}R_R}. \qquad (E29)$$

Note that in a similar manner to that used in Appendix D, equation (E29) can be put in the form:

$$e_{c_1} - e_{c_2} = \frac{K_2 N_c^2 V_c}{R_c + K_2 N_c^2} , \tag{E30}$$

where

$$K_2 = \frac{R_R}{N_s^2} . \tag{E31}$$

The time t_6 can be found by solving equations (E23) through (E28) for the voltage e_{c_2} and equating it to zero to find time t_6 such that $\pi/2\omega < t_6 < {}^2\pi/\omega$.

$$t_6 = \frac{\pi}{\omega} - t_5 . \tag{E32}$$

9. The flux difference produced between the levels in the two reactors during the interval of time $t_5 < t < t_6$ is found from Faraday's Law:

$$\Delta\phi_2 = \frac{1}{N_2}\int_{t_5}^{t_6} (e_{c_1} - e_{c_2})\, dt . \tag{E33}$$

Evaluating the integral using equation (E30) gives:

$$\Delta\phi_2 = \frac{K_2 N_c}{R_c + K_2 N_c^2} V_c \left(\frac{\pi}{\omega} - 2t_5\right) . \tag{E34}$$

Substituting the time t_5 from equation (E19) and using the identity:

$$\cos^{-1} a = \frac{\pi}{2} - \sin^{-1} a , \tag{E35}$$

Equation (E34) becomes:

$$\Delta\phi_2 = \frac{2}{\omega} \frac{K_2 N_c}{R_c + K_2 N_c^2} V_c \cos^{-1}(\alpha_0 + \alpha_2 V_c) . \tag{E36}$$

10. After the time t_6 the operation of reactor 1 continues down the side of the loop toward point f in figure 12, while the operation of reactor 2 goes from point e toward point g in the same figure. Defining time t_7 as the time at which reactor 1 reaches point f of figure 12,

the equivalent circuit for the time interval $t_6 < t < t_7$ is once again that shown in figure 17 with equations (E10) through (E14) describing the circuit. During this interval of time there is no flux change produced in reactor 2, while in reactor 1 a flux change $\Delta \phi_1$ occurs which is the same as that occurring during the interval $t_4 < t < t_5$. This can be shown to be true by solution of the appropriate equations or by physical reasoning.

11. At the time t_7, found to be

$$t_7 = \frac{\pi}{\omega} - t_4. \tag{E37}$$

reactor 1 reaches point f on the loop of figure 12. During the interval of time $t_7 < t < \pi/\omega$, no flux change occurs in either reactor; consequently the net flux change produced between the levels in the two reactors during the reset half-cycle due to a control voltage V_c is:

$$\Delta\phi = 2\Delta\phi_1 + \Delta\phi_2, \tag{E38}$$

where $\Delta \phi_1$ is given by equation (E22) and $\Delta \phi_2$ by equation (E36). Substitution of these values into equation (E38) yields:

$$\Delta\phi = \frac{K_2 N_c}{R_c + K_2 N_c^2} \frac{2V_c}{\omega} \cos^{-1}(\alpha_0 + \alpha_2 V_c)$$

$$+ \frac{V_s}{\omega N_1} \frac{\left(1 + \frac{N_s}{N_1}\frac{R_b}{R_s}\right)}{\beta_1} \left\{ \cos \sin^{-1}(\alpha_0 - \alpha_1 V_c) - \cos \sin^{-1}(\alpha_0 + \alpha_2 V_c) \right.$$

$$\left. + \left(\frac{\frac{N_c}{N_1}\frac{R_b}{R_s}\frac{V_c}{V_s}}{1 + \frac{N_s}{N_1}\frac{R_b}{R_s}} - \alpha_0 \right) \left[\sin^{-1}(\alpha_0 + \alpha_2 V_c) - \sin^{-1}(\alpha_0 - \alpha_1 V_c) \right] \right\}. \tag{E39}$$

Note that for small signals ($V_c \longrightarrow 0$) equation (E39) reduces to:

$$\Delta\phi = \frac{K_2 N_c}{R_c + K_2 N_c^2} \frac{2V_c}{\omega} \cos^{-1}\alpha_o. \qquad \text{(E40)}$$

This demonstrates that for small signals the flux difference $\Delta\,\phi$ is a linear function of the control voltage.

APPENDIX F

ANALYSIS DURING OPERATING HALF-CYCLE OF BOTH CIRCUITS FOR DIRECT CONTROL VOLTAGE, V_c

1. In order to draw an equivalent circuit for the half-wave bridge magnetic amplifier for operation during the operating half-cycle, a number of assumptions must be made. The assumptions apply to both circuits of figure 1.

a. The saturated impedance of each arm of the bridge (resistance of one power winding plus the forward resistance of one rectifier) is denoted R_f and is assumed resistive.

b. The voltage drops across the rectifier forward resistances and the load resistance due to reactor exciting currents are negligible.

c. The reset circuits have no effect on the circuit; hence they can be disregarded during this half-cycle of operation.

d. When load current flows, it is very large compared to the exciting current.

e. The control circuit presents a sufficiently high impedance to the load circuit that it can be disregarded.

2. Using the above assumptions the equivalent circuit for both figures 1(a) and 1(b) is shown in figure 19 for the time interval $0 < t < t_8$ where t_8 is defined as the time at which the operation of reactor 2 reaches point i in figure 12. During this interval the reactor fluxes change at the same rate; therefore, when the operation of reactor 2 reaches point i in figure 12 ($t = t_8$), an amount of flux $\Delta \phi$ must be changed in reactor 1 before it, too, reaches point i. The time at which this occurs is defined as t_9.

3. During the time interval $t_8 < t < t_9$ current is delivered to the load. The equivalent circuit for this time interval is given in figure 20. In view of assumption (d) above, by simple voltage division:

$$e_s = \frac{R_L + R_f}{R_L + 2R_f + R_s} V_s \,, \tag{F1}$$

and

$$V_L = \frac{R_L}{R_L + 2R_f + R_s} V_s \,. \tag{F2}$$

The flux change in reactor 1 during the time interval $t_8 < t < t_9$ is, by Faraday's Law:

$$\Delta\phi = \frac{1}{N_s}\int_{t_8}^{t_9} e_s \, dt \,, \tag{F3}$$

While the average value of the load voltage is:

$$V_L = \frac{\omega}{2\pi}\int_{t_8}^{t_9} v_L \, dt \,. \tag{F4}$$

Substituting equation (F1) into (F3) and (F2) into (F4) gives:

$$\Delta\phi = \frac{1}{N_s}\left(\frac{R_L + R_f}{R_L + 2R_f + R_s}\right)\int_{t_8}^{t_9} V_s \sin \omega t \, dt \,, \tag{F5}$$

and

$$V_L = \frac{\omega}{2\pi}\left(\frac{R_L}{R_L + 2R_f + R_s}\right)\int_{t_8}^{t_9} V_s \sin \omega t \, dt. \tag{F6}$$

Elimination of the integral between equations (F5) and (F6) leads to:

$$V_L = \frac{\omega}{2\pi} N_s \left(\frac{R_L}{R_L + R_f}\right)\Delta\phi \,. \tag{F7}$$

This is a gain equation describing the operation of the circuit during the operating half-cycle because the input on this half-cycle is the flux difference $\Delta\,\phi$, while the output is the load voltage V_L.

APPENDIX G

GAIN EQUATIONS AND OPTIMIZATION OF CONTROL CIRCUIT WITH PARALLEL RESET

1. Combining equations (D42) of Appendix D and (F7) of Appendix F gives the average load voltage V_L as a function of the direct control voltage V_c:

$$V_L = \left(\frac{R_L}{R_L+R_f}\right)\left[\frac{K_1 N_c}{R_c+K_1 N_c^2}\,\frac{N_s V_s}{\pi}\cos^{-1}(\alpha_0+\alpha_2 V_c)\right.$$

$$+\frac{N_s}{N_r}\,\frac{V_s}{2\pi}\,\frac{1+\frac{N_s}{N_r}\frac{R_b}{R_R}}{\beta_1}\left\{\cos\sin^{-1}(\alpha_0-\alpha_1 V_c)-\cos\sin^{-1}(\alpha_0+\alpha_2 V_c)\right.$$

$$\left.\left.+\left(\frac{\frac{N_s}{N_r}\frac{R_b}{R_c}\frac{V_c}{V_s}}{1+\frac{N_s}{N_r}\frac{R_b}{R_R}}-\alpha_0\right)\left[\sin^{-1}(\alpha_0+\alpha_2 V_c)-\sin^{-1}(\alpha_0-\alpha_1 V_c)\right]\right\}\right]. \qquad (G1)$$

This equation indicates the types and magnitudes of non-linearities in the transfer function of this amplifier even when "ideal" components are assumed.

2. In a practical amplifier of this type there is a good usable range of output levels over which the gain is very nearly constant. Also, in servo applications the gain of interest in studying stability is the gain near zero control voltage. In this region the expression of equation (G1) simplifies to:

$$\frac{V_L}{V_c}=\left(\frac{R_L}{R_L+R_f}\right)\left(\frac{K_1 N_c}{R_c+K_1 N_c^2}\right)\frac{N_s}{\pi}\cos^{-1}\alpha_0. \qquad (G2)$$

Good design information can be obtained by studying this expression.

3. Inspection of equations (D7) and (D34) of Appendix D shows that neither K_1 nor α_o is a function of the control turns N_c; therefore the expression given in equation (G2) can be maximized with respect to N_c by taking the partial derivative of the expression with respect to N_c and equating to zero thus:

$$0 = \frac{\partial\left(\frac{V_L}{V_s}\right)}{\partial N_c} = \left(\frac{R_L}{R_L+R_f}\right)\left[\frac{K_1(R_c+K_1N_c^2)-K_1N_c(2K_1N_c)}{R_c+K_1N_c^2}\right]\frac{N_s}{\pi}\cos^{-1}\alpha_o . \qquad (G3)$$

Solution of this expression for N_c yields:

$$N_c = \sqrt{\frac{R_c}{K_1}} . \qquad (G4)$$

Substitution of this value for N_c into equation (G2) gives:

$$\frac{V_L}{V_s} = \left(\frac{R_L}{R_L+R_f}\right)\sqrt{\frac{K_1}{R_c}}\,\frac{N_s}{2\pi}\cos^{-1}\alpha_o . \qquad (G5)$$

This equation holds true so long as N_c is adjusted according to equation (G4), in which case this is the maximum attainable gain if all the parameters except N_c are fixed.

4. The optimization of this expression with respect to the other parameters is quite involved. The effect of each one on the gain can be investigated but it is rather difficult to derive simple conditions like that for the control turns above.

5. If the power gain of the d-c component of the output is desired, this can be obtained from equation (G5) thus:

$$\frac{V_L^2}{R_L}\,\frac{R_c}{V_c^2} = \frac{R_L}{(R_L+R_f)^2}K_1\frac{N_s^2}{4\pi^2}\left(\cos^{-1}\alpha_o\right)^2 . \qquad (G6)$$

Note that this expression is independent of the control circuit parameters. Thus, with the design of the power and reset circuits and with the control turns adjusted according to equation (G4), equation (G6) gives the maximum obtainable power gain through the circuit.

APPENDIX H

GAIN EQUATIONS AND OPTIMIZATION OF CONTROL CIRCUIT WITH SERIES RESET

1. Combining equations (E39) of Appendix E and equation (F7) of Appendix F gives the average load voltage V_L as a function of the direct control voltage V_c:

$$V_L = \left(\frac{R_L}{R_L+R_f}\right)\left[\frac{K_2 N_c}{R_c+K_2 N_c^2}\,\frac{N_s V_c}{\pi}\cos^{-1}(\alpha_0+\alpha_3 V_c)\right.$$

$$+\frac{N_s}{N_r}\,\frac{V_s}{2\pi}\,\frac{\left(1+\frac{N_s}{N_r}\frac{R_b}{R_R}\right)}{\beta_1}\left\{\cos\sin^{-1}(\alpha_0-\alpha_1 V_c)-\cos\sin^{-1}(\alpha_0+\alpha_3 V_c)\right.$$

$$\left.\left.+\left(\frac{\frac{N_s}{N_r}\frac{R_b}{R_c}\frac{V_c}{V_s}}{1+\frac{N_s}{N_r}\frac{R_b}{R_R}}-\alpha_0\right)\left[\sin^{-1}(\alpha_0+\alpha_3 V_c)-\sin^{-1}(\alpha_0-\alpha_1 V_c)\right]\right\}\right]. \qquad (H1)$$

Note that except for the definitions of K_2 and α_3 this expression is the same as equation (G1) of Appendix G for the circuit with parallel reset.

2. For small signals ($V_c \longrightarrow 0$), equation (H1) simplifies to:

$$\frac{V_L}{V_c} = \left(\frac{R_L}{R_L+R_f}\right)\left(\frac{K_2 N_c}{R_c+K_2 N_c^2}\right)\frac{N_s}{\pi}\cos^{-1}\alpha_0. \qquad (H2)$$

This is the same form as equation (G2) of Appendix G; hence, to adjust the control turns for optimum gain, the control turns must be adjusted according to:

$$N_c = \sqrt{\frac{R_c}{K_2}}. \qquad (H3)$$

Substitution of this value into equation (H2) yields:

$$\frac{V_L}{V_c} = \left(\frac{R_L}{R_L + R_f}\right)\sqrt{\frac{K_2}{R_c}}\,\frac{N_s}{2\pi}\cos^{-1}\alpha_o . \qquad \text{(H4)}$$

This equation holds true when N_c is adjusted according to equation (H3). If all other parameters except N_c are fixed, this expression gives the maximum gain obtainable.

3. The optimization of the rest of the parameters is complicated but the effect of each one on the circuit can be found by studying the expressions given. No simple expressions like that for control turns can be derived for the other components.

4. The power gain to the d-c component of the output is:

$$\left(\frac{V_L}{V_c}\right)^2 \frac{R_c}{R_L} = \frac{R_L}{(R_L + R_f)^2} K_2 \frac{N_s^2}{4\pi^2}\left(\cos^{-1}\alpha_o\right)^2 . \qquad \text{(H5)}$$

This expression is independent of control circuit parameters, showing that when everything but the control circuit is fixed there is a maximum power gain obtainable through the circuit which is independent of the impedance level of the control circuit so long as the control turns N_c are adjusted according to equation (H3).

REFERENCES

1. "An Improved Magnetic Servo Amplifier", C. W. Lufcy, A. E. Schmid, P. W. Barnhart, A.I.E.E. Technical Paper 52-235, May 1952, A.I.E.E. Transactions, September 1952.

2. "A Half-Wave Auto-Transformer Magnetic Amplifier", E. T. Hooper, NavOrd Report 2719, January 1953.

3. "Design Considerations of the Half-Wave Bridge Magnetic Amplifier", C. W. Lufcy and H. H. Woodson, A.I.E.E. Technical Paper 54-182, January 1954.

4. "Compensation of a Magnetic Amplifier Servo System", H. H. Woodson, A. E. Schmid, C. V. Thrower, Proceedings of the National Electronics Conference, 1952.

5. "Magnetic Amplifier Servo Compensation", H. H. Woodson, NavOrd Report 2709, December 1952.

6. "Magnetic Control Amplifiers XM-16A and XM-17A for Use with Servo Motors Mk 7, Mk 8, Mk 14 and Mk 16", E. T. Hooper, NavOrd Report 2833, May 1953.

7. "Lead-Lag and Lead-Integral Servo Compensation Using Half-Wave Bridge Magnetic Amplifiers", H. H. Woodson, L. S. Weinstein and J. E. Roberts, NavOrd Report 3560, January 1954.

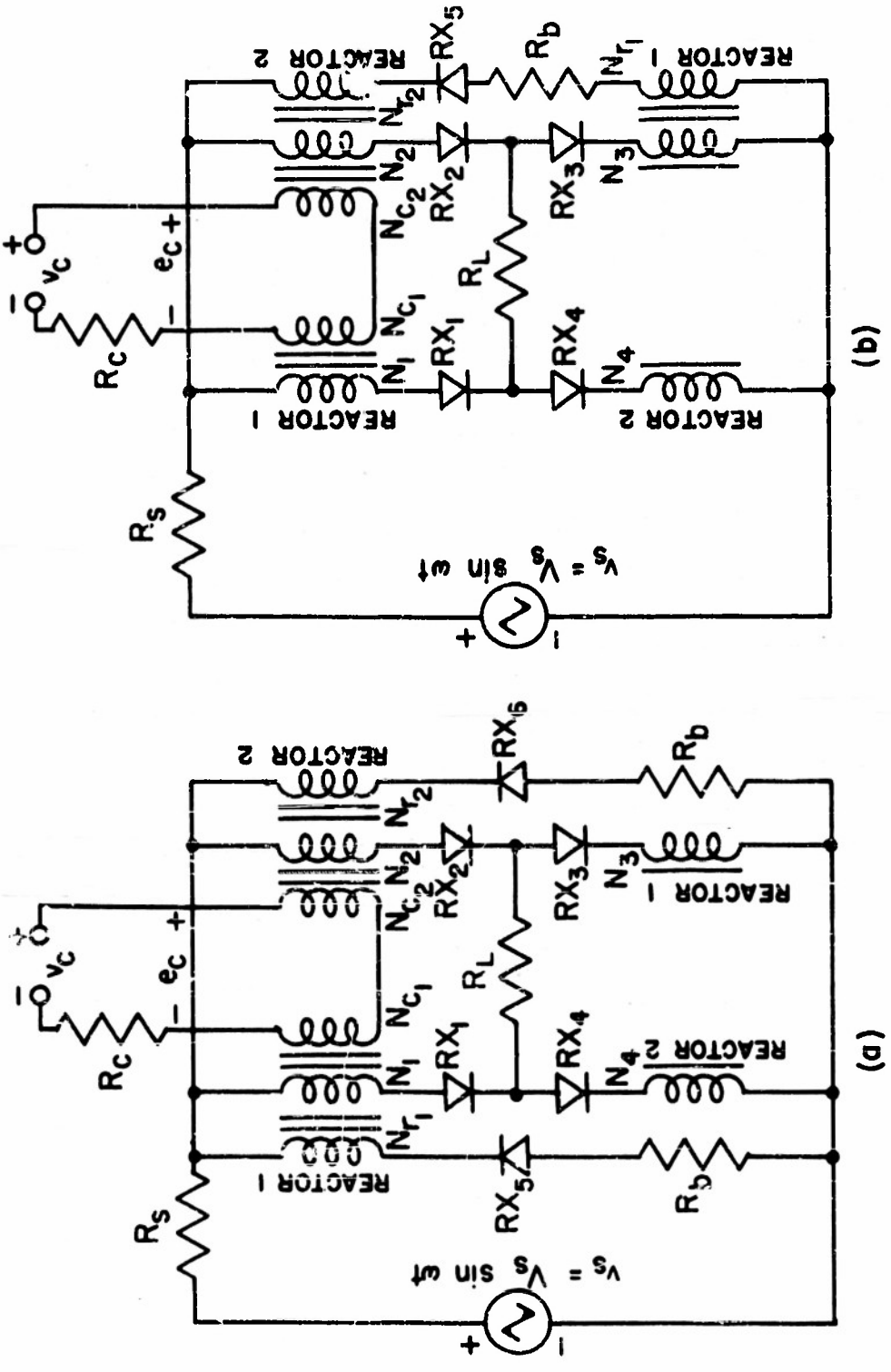

FIG. 1 - HALF-WAVE BRIDGE MAGNETIC AMPLIFIER CIRCUITS

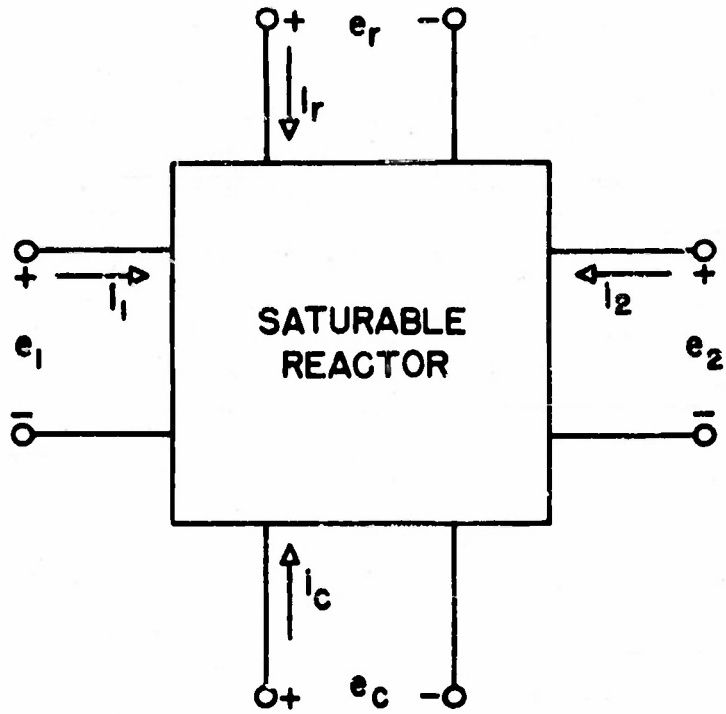

FIG. 2 – EQUIVALENT CIRCUIT OF SATURABLE REACTOR

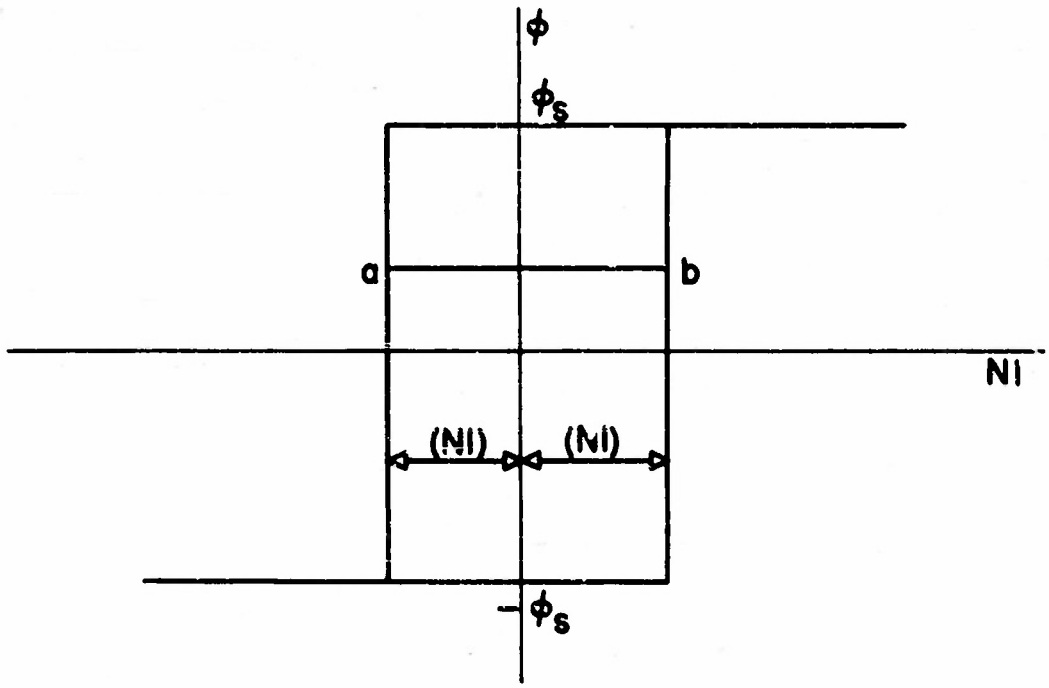

FIG. 3 – FLUX–MMF LOOP OF REACTOR

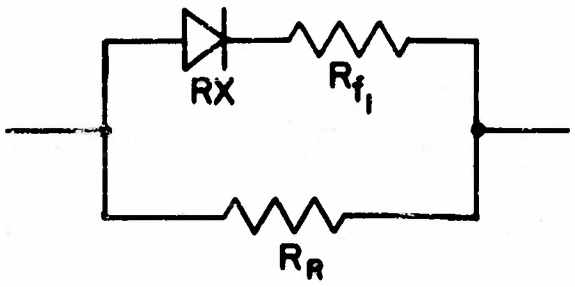

FIG. 4 — EQUIVALENT CIRCUIT OF RECTIFIER

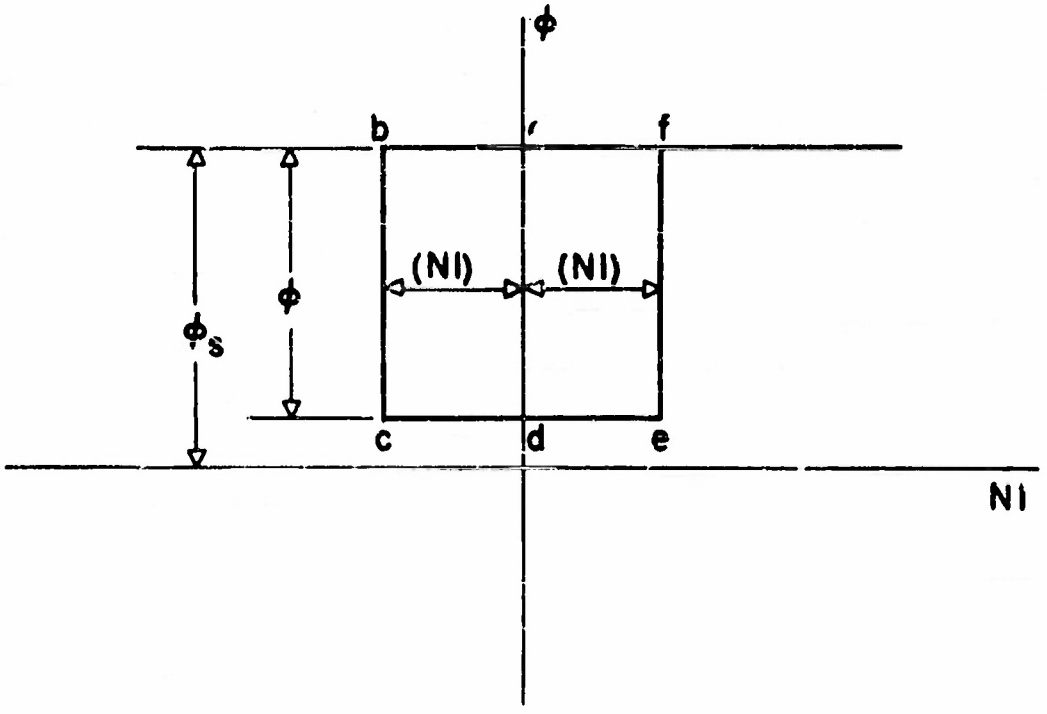

FIG. 5 — OPERATING FLUX—MMF LOOPS UNDER QUIESCENT CONDITIONS

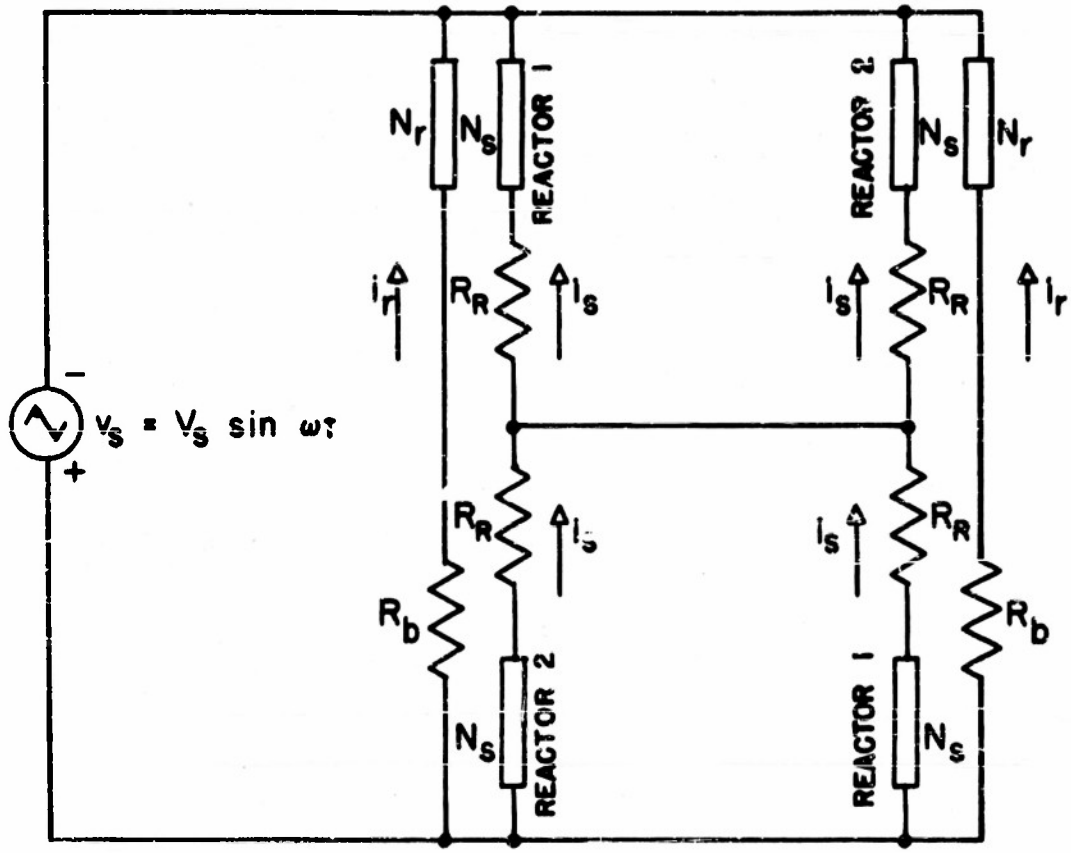

FIG. 6 – EQUIVALENT CIRCUIT WITH PARALLEL RESET – RESET HALF-CYCLE – QUIESCENT CONDITIONS AND BOTH REACTORS SATURATED

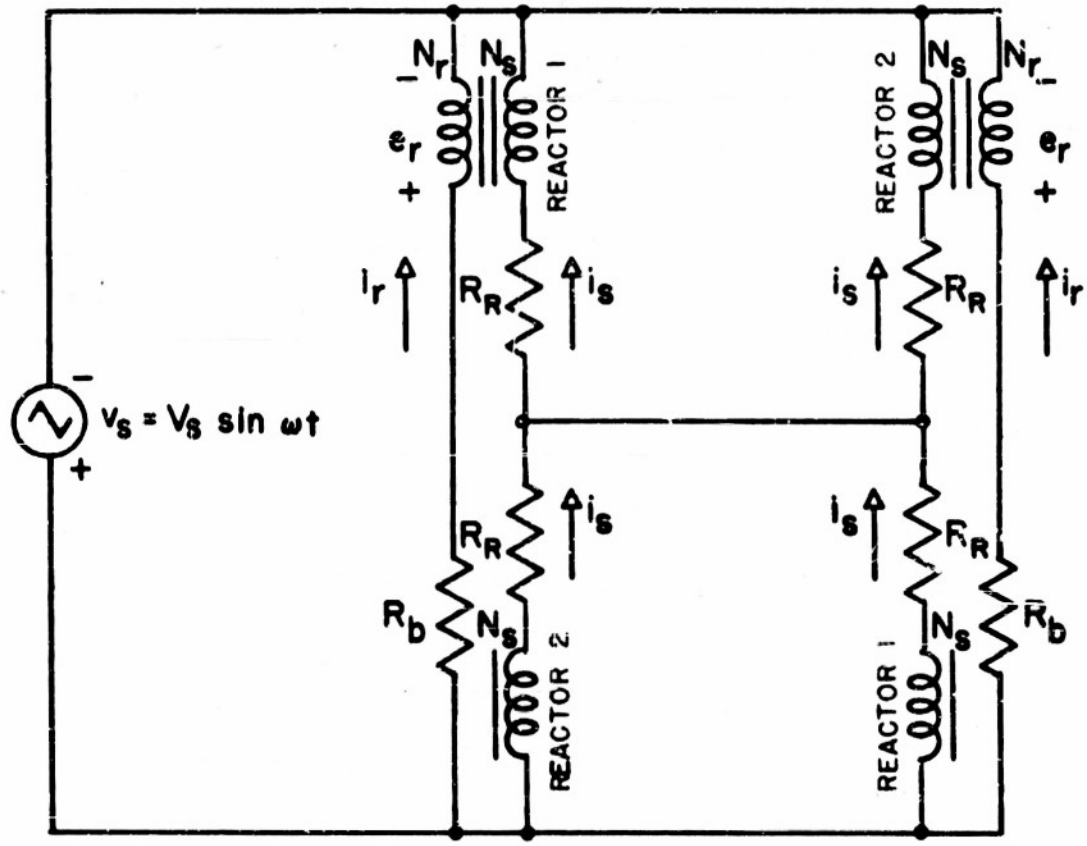

FIG. 7 — EQUIVALENT CIRCUIT WITH PARALLEL RESET — RESET HALF-CYCLE — QUIESCENT CONDITIONS AND BOTH REACTORS UNSATURATED

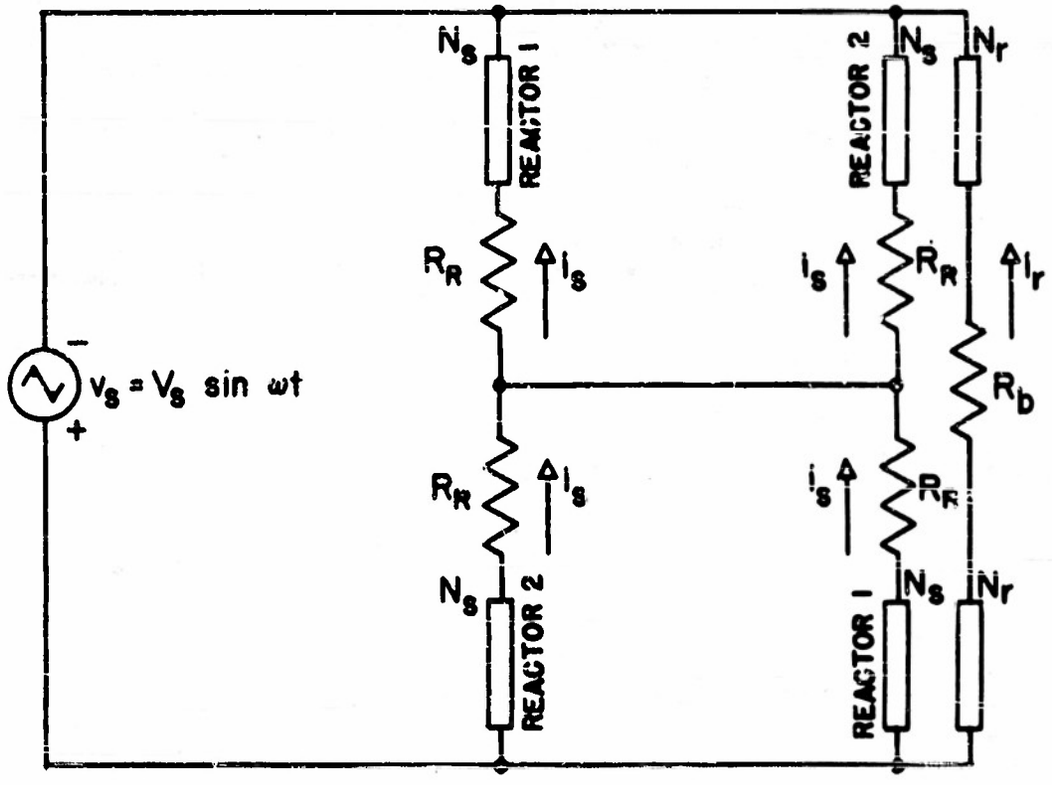

FIG. 8 – EQUIVALENT CIRCUIT WITH SERIES RESET — RESET HALF-CYCLE — QUIESCENT CONDITIONS AND BOTH REACTORS SATURATED

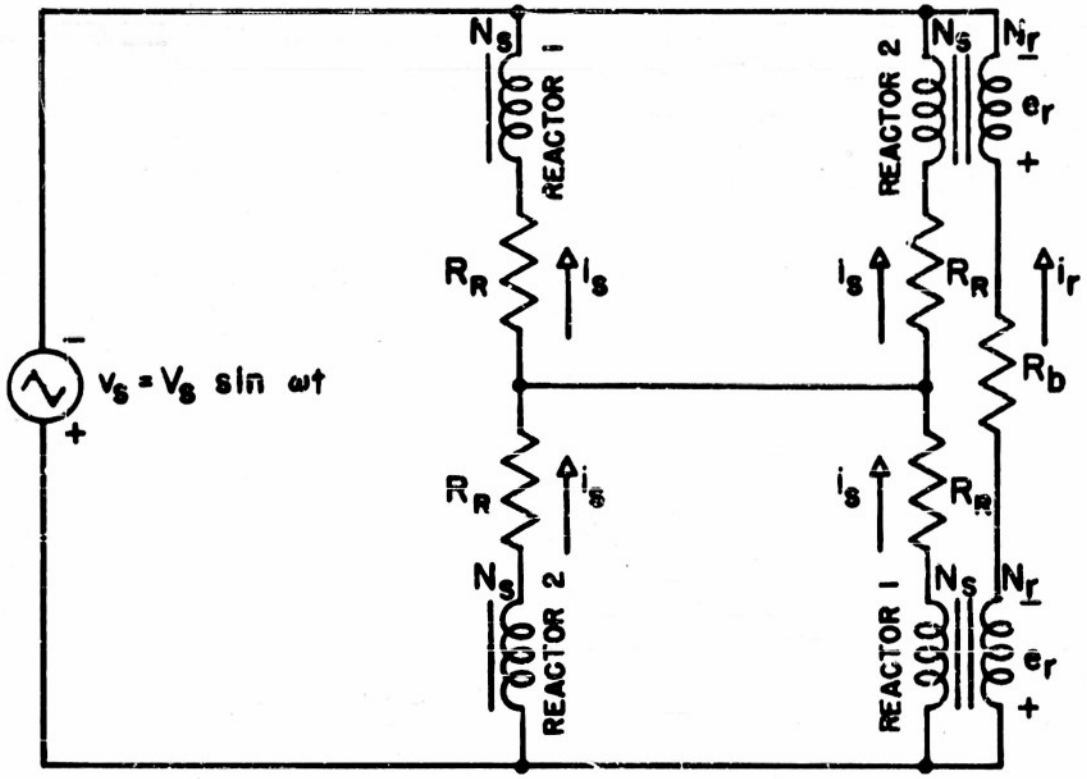

FIG. 9 — EQUIVALENT CIRCUIT WITH SERIES RESET — RESET HALF-CYCLE — QUIESCENT CONDITIONS AND BOTH REACTORS UNSATURATED

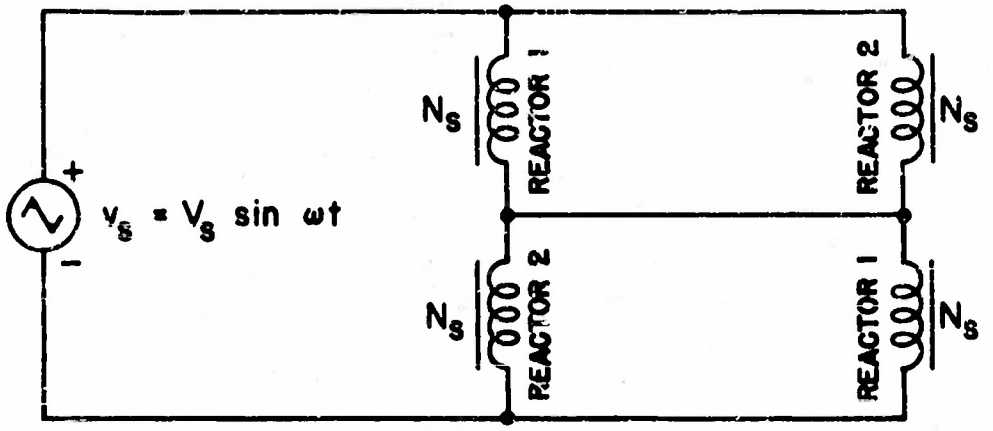

FIG. 10 — EQUIVALENT CIRCUIT — OPERATING HALF-CYCLE — QUIESCENT CONDITIONS — BOTH REACTORS UNSATURATED

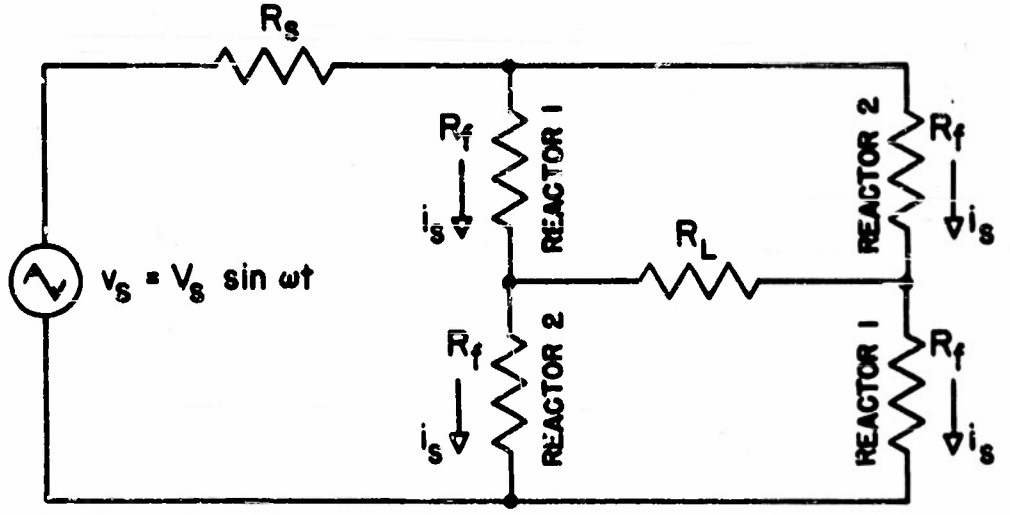

FIG. 11 — EQUIVALENT CIRCUIT — OPERATING HALF-CYCLE — QUIESCENT CONDITIONS — BOTH REACTORS SATURATED

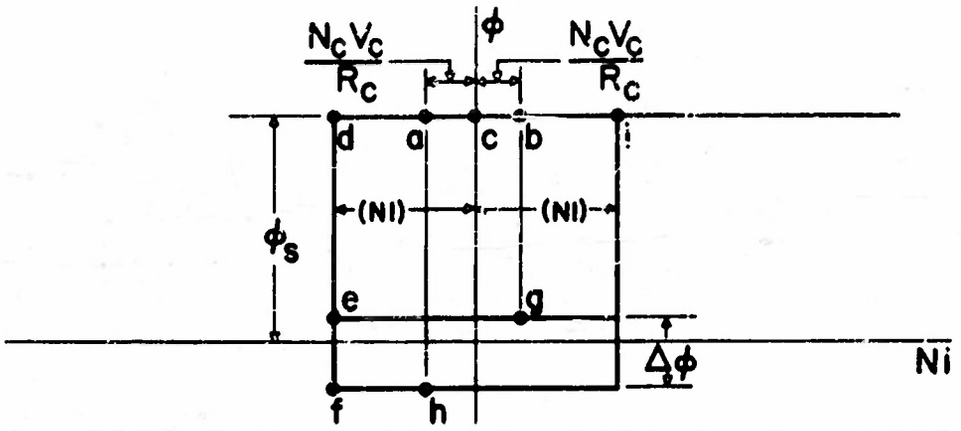

FIG. 12 — OPERATING FLUX-MMF LOOPS OF REACTORS WITH CONTROL SIGNAL

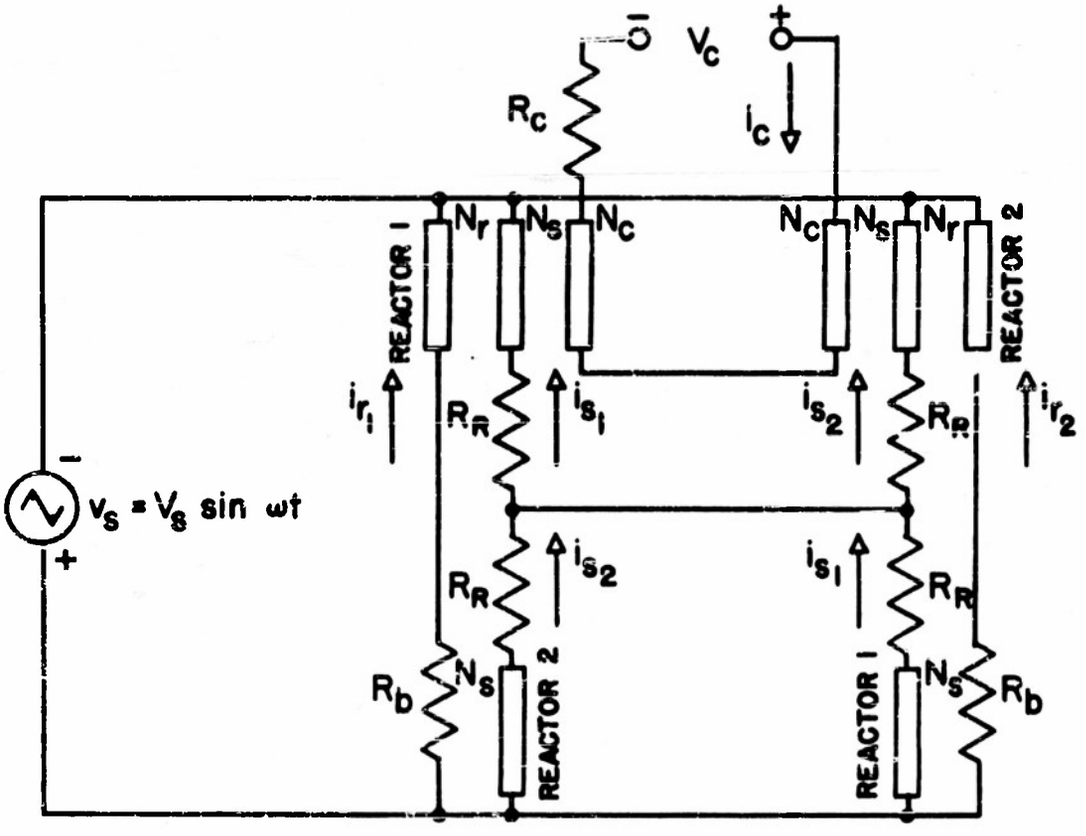

FIG. 13 — EQUIVALENT CIRCUIT WITH PARALLEL RESET — RESET HALF-CYCLE — SIGNAL CONDITIONS AND BOTH REACTORS SATURATED

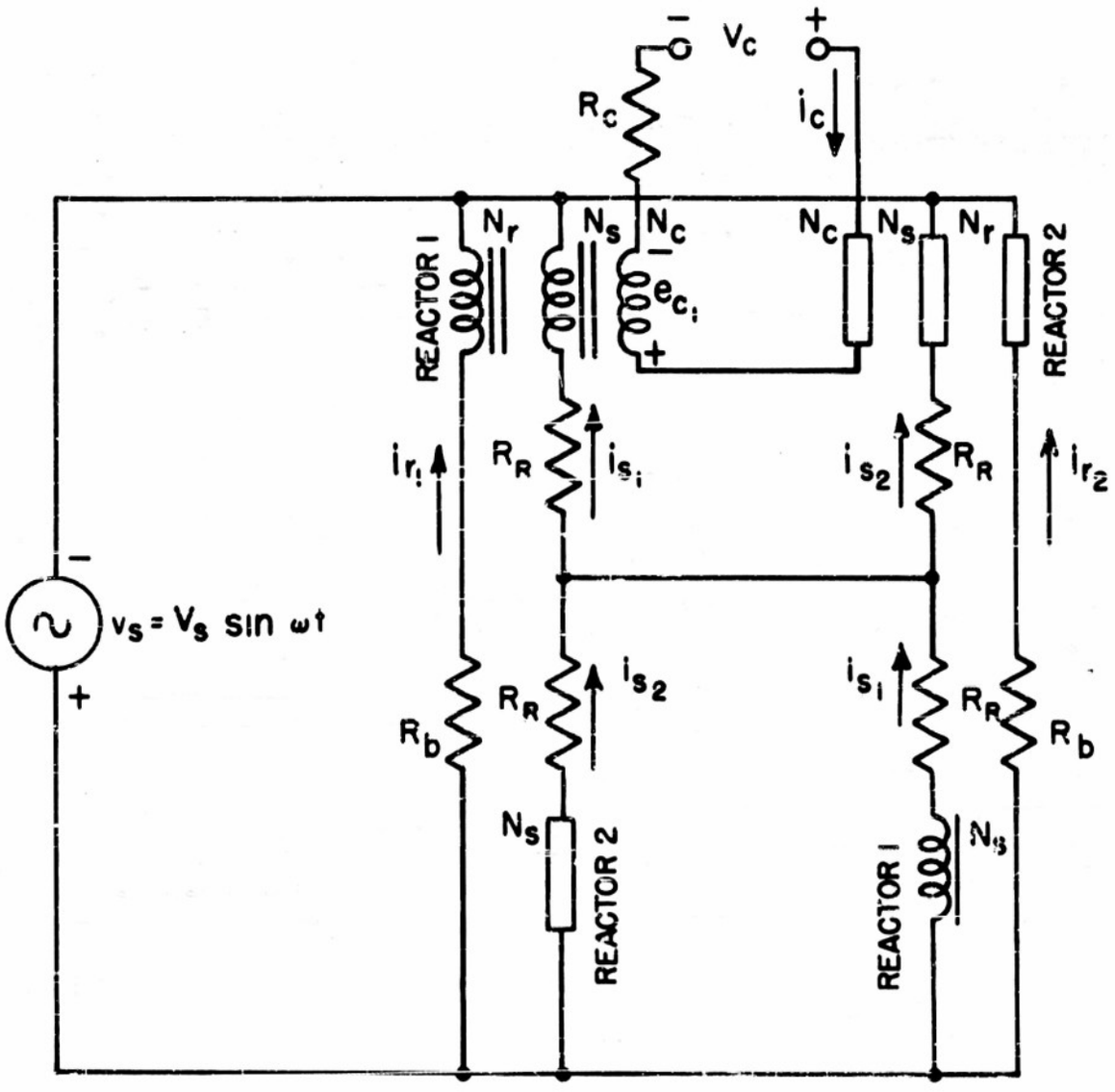

FIG. 14 EQUIVALENT CIRCUIT WITH PARALLEL RESET — RESET HALF CYCLE — SIGNAL CONDITIONS AND ONE REACTOR SATURATED

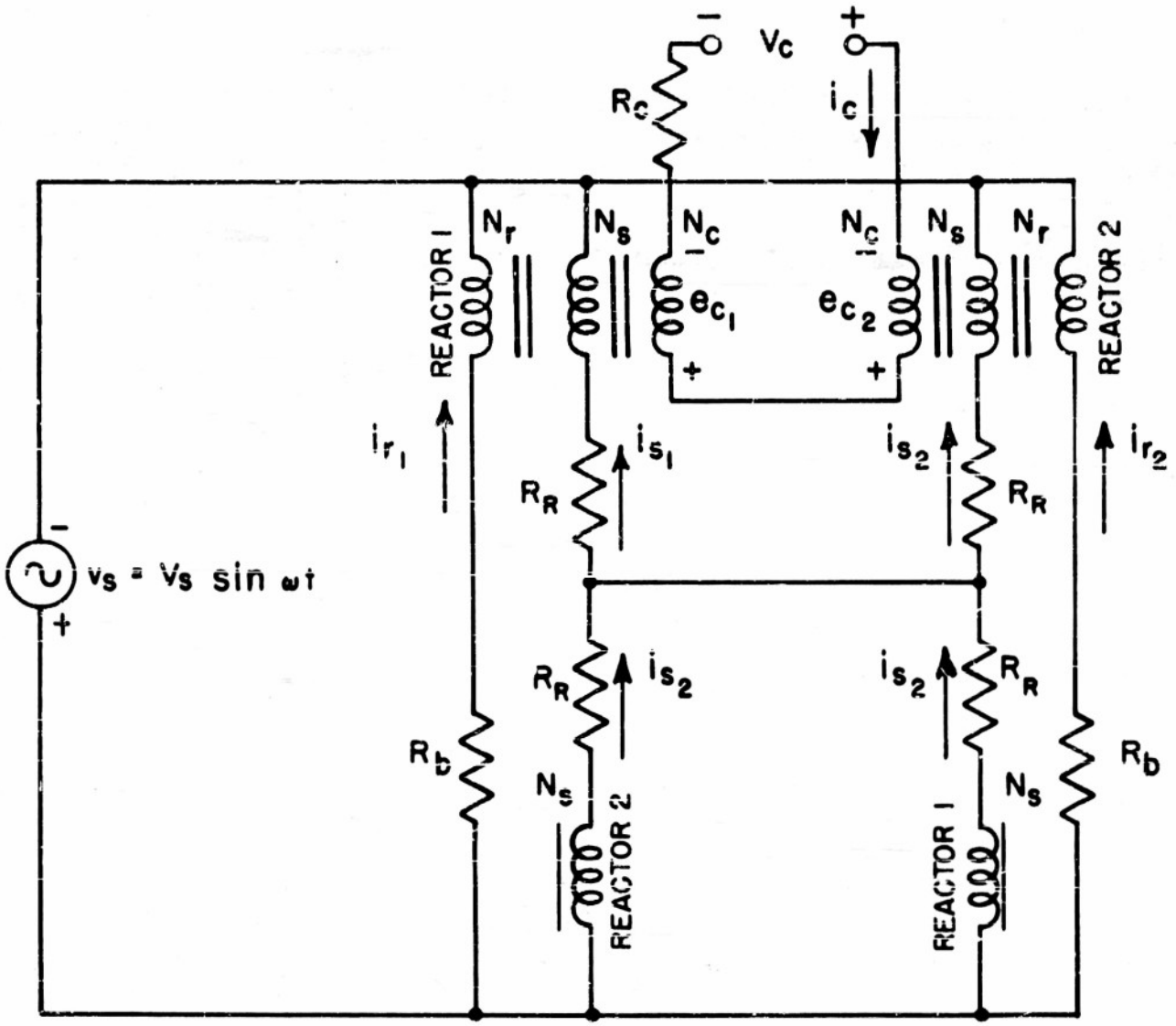

FIG. 15 EQUIVALENT CIRCUIT WITH PARALLEL RESET—RESET HALF-CYCLE—SIGNAL CONDITIONS AND BOTH REACTORS UNSATURATED

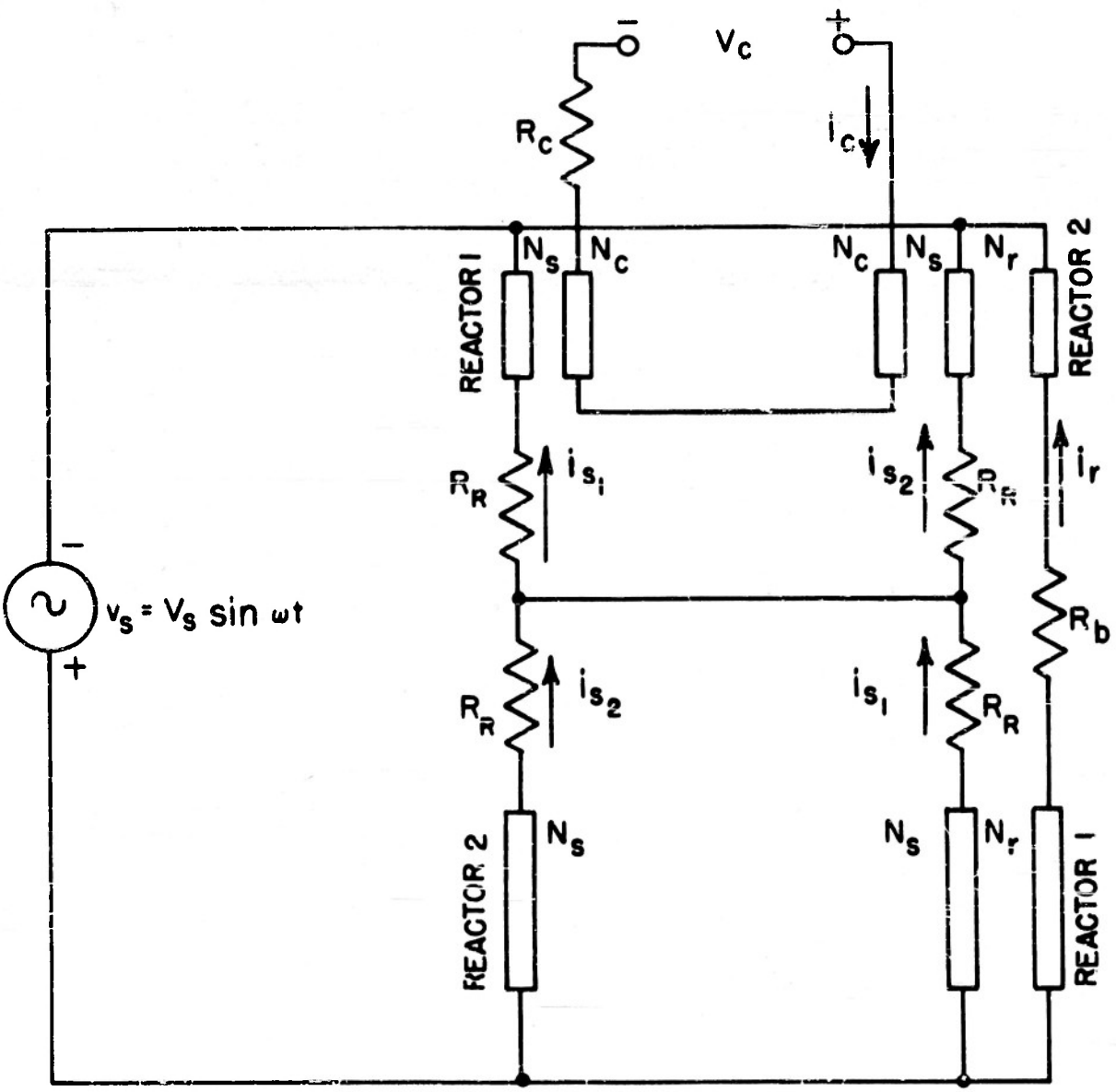

FIG. 16 EQUIVALENT CIRCUIT WITH SERIES RESET — RESET HALF - CYCLE — SIGNAL CONDITIONS AND BOTH REACTORS SATURATED

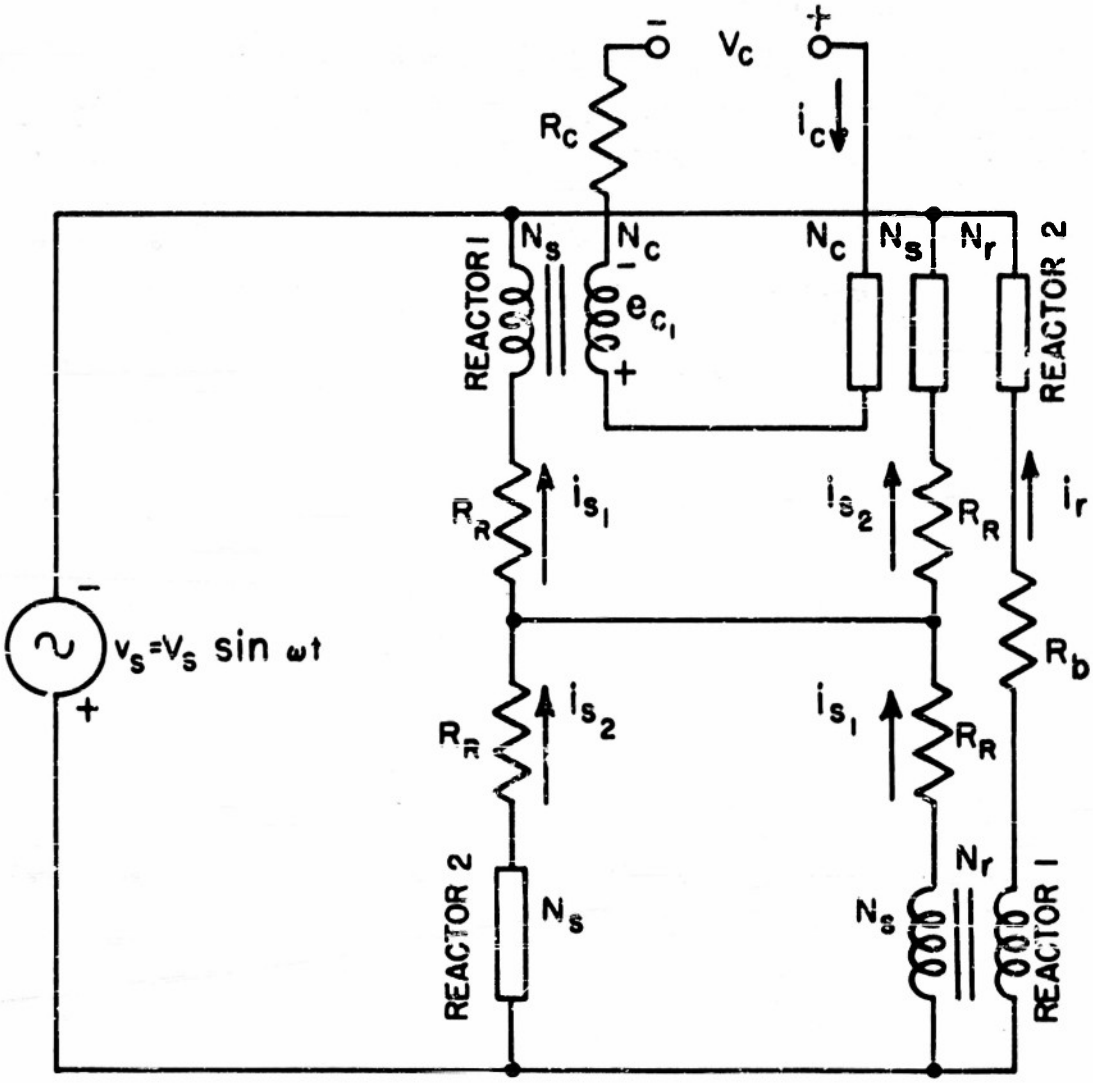

FIG. 17 EQUIVALENT CIRCUIT WITH SERIES RESET— RESET HALF-CYCLE — SIGNAL CONDITIONS AND ONE REACTOR SATURATED

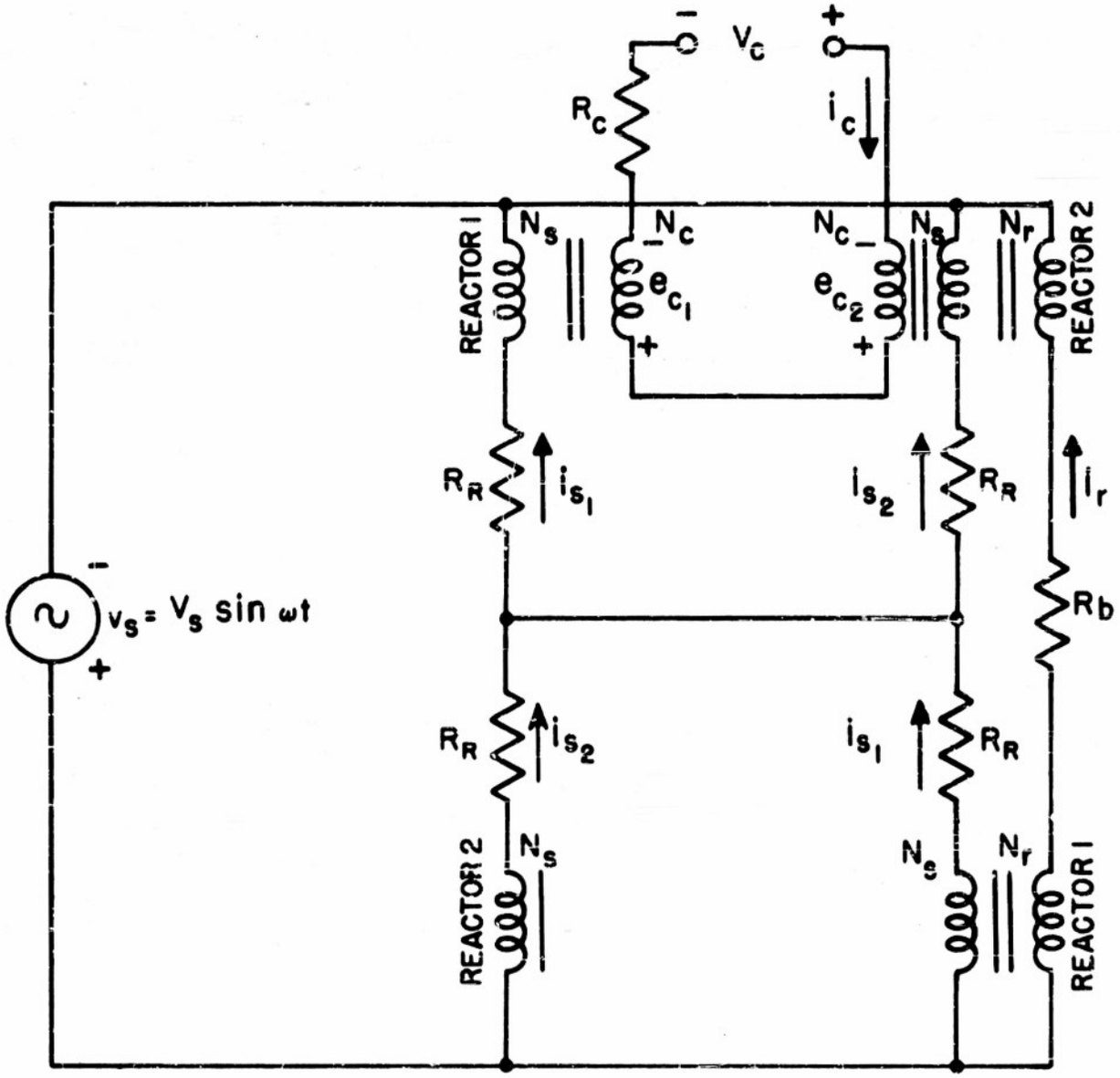

FIG. 18 EQUIVALENT CIRCUIT WITH SERIES RESET — RESET HALF-CYCLE — SIGNAL CONDITIONS AND BOTH REACTORS UNSATURATED

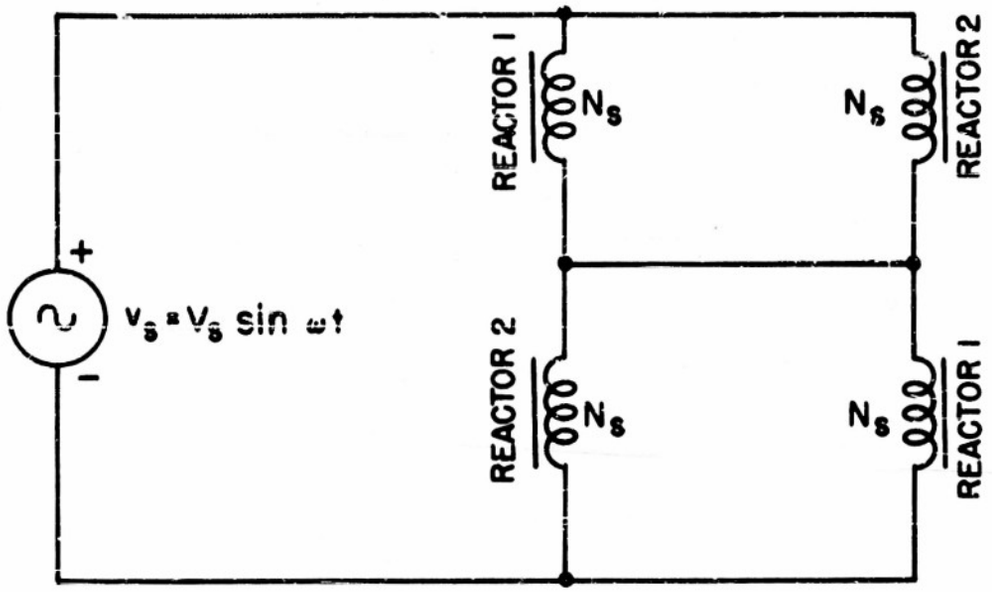

FIG. 19 EQUIVALENT CIRCUIT — OPERATING HALF-CYCLE — SIGNAL CONDITIONS — BOTH REACTORS UNSATURATED

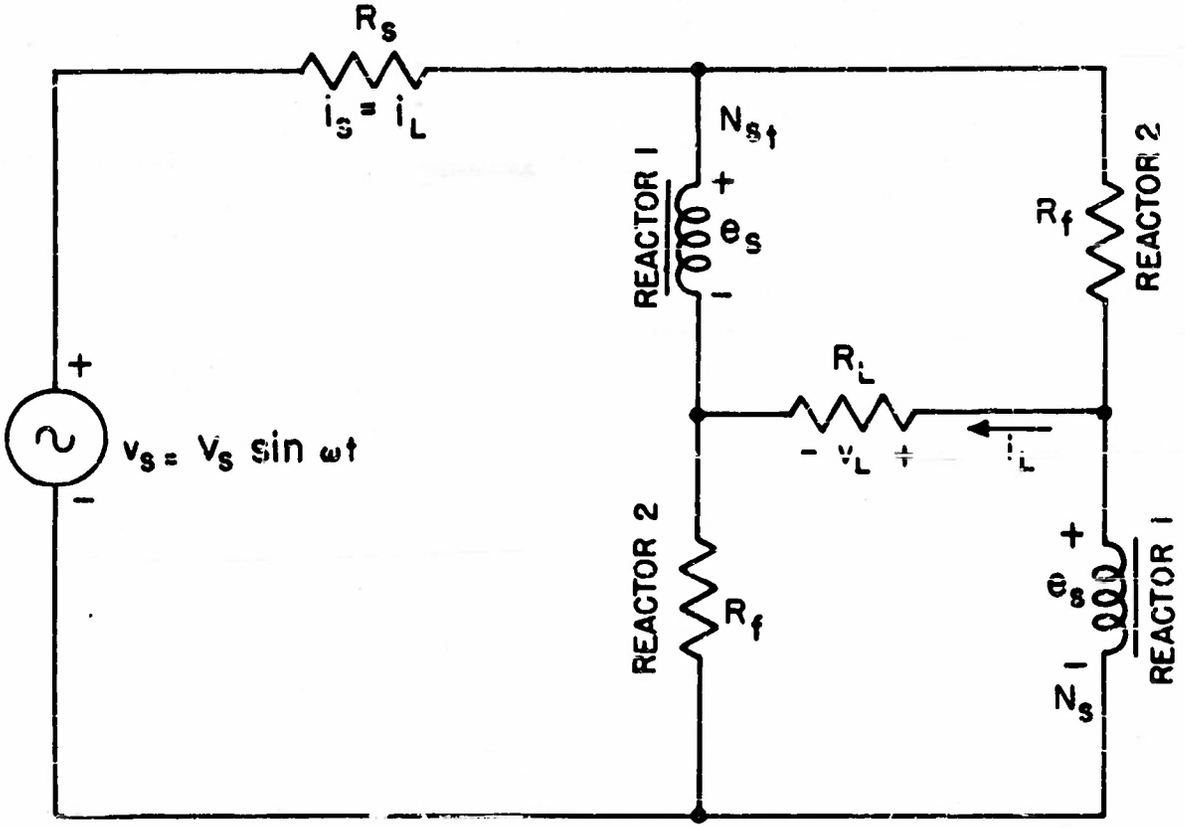

FIG. 20 EQUIVALENT CIRCUIT WHILE CURRENT IS FLOWING IN LOAD

DISTRIBUTION

	Copies
Chief, Bureau of Ordnance	
H. B. Rex (Re4-3)	1
N. J. Smith (Re4a)	1
J. L. Miller (Re8-5)	1
W. B. Ensinger (Re8-2)	1
A. A. Powell (Re4b)	1
Chief, Bureau of Ships	
Code 343	1
J. Watkins (560E)	1
Commanding Officer, Naval Air Missile Test Center, Point Mugu, California	
Attention Dr. Royal Weller	1
Commanding Officer, U. S. Naval Ordnance Plant, Indianapolis, Indiana	
Attention R. E. Williams, Radar Division	1
Senior Naval Liaison Officer, U. S. Navy Electronics Office, Fort Monmouth, New Jersey	1
Commanding Officer, U. S. Naval Ordnance Test Station, 3202 E. Foothill Boulevard, Pasadena 8, California	
Attention Robert R. Selin (Code P8045)	1
Director, Navy Electronics Laboratory, San Diego, California	
Attention Robert L. Ogram	1
Commanding General, Wright Air Development Center, Wright-Patterson Air Force Base, Dayton, Ohio	
Attention WCRSD-5	1
WCERG-2	1
R. M. Wundt, WCLGD-2	1
Director, David Taylor Model Basin, Washington 25, D. C.	
Attention S. Edward Dawson	1
Director, Naval Research Laboratory, Washington 25, D. C.	
Attention John Hart, Electricity Division	1
Rome Air Development Center (RCR), Griffiss Air Force Base, Rome, New York	
Attention Philip Zirkind (RCRTR-5)	1
Commanding General, Frankfort Arsenal, Box 7989, Philadelphia 1, Pennsylvania	
Attention Donald Brown (PEL)	1

	Copies
Arma Corporation, Garden City, Long Island, New York	
Attention Engineering Division	1
Librascope, Incorporated, 1607 Flower Street, Glendale 1, California	
Attention Engineering Division	1
Vitro Corporation of America, 962 Wayne Avenue, Silver Spring, Maryland	
Attention Librarian	1
Sperry Gyroscope Company, Division of the Sperry Corporation, Great Neck, Long Island, New York	
Attention Special Armament Systems Department	1
Massachusetts Institute of Technology, Cambridge 39, Massachusetts	
Attention Professor G. C. Newton, Jr., Servomechanisms Laboratory, Building 32	1
Professor E. W. Boehne, Room 4-207	1
Professor D. C. White, Electrical Engineering Department, Room 10-198	1
Mr. H. H. Woodson, Servomechanisms Laboratory, Building 32	1
Illinois Institute of Technology, 3300 S. Federal Street, Chicago, Illinois	
Attention Dr. P. L. Copeland, Head, Department of Physics	1
Illinois Institute of Technology, Technology Center, Chicago 16, Illinois	
Attention Mr. L. C. Labarthe, Electrical Engineering Research, Armour Research Foundation	1
Yale University, Department of Electrical Engineering, 10 Hillhouse Avenue, New Haven, Connecticut	
Attention Professor J. C. May	1
University of Wisconsin, Madison 6, Wisconsin, Department of Electrical Engineering, Engineering Building	
Attention Professor T. J. Higgens	1
University of California, Berkeley 4, California, College of Engineering, Division of Electrical Engineering	
Attention Professor O. J. M. Smith	1
Purdue University, Lafayette, Indiana, School of Electrical Engineering	
Attention E. M. Sabbagh	1
Applied Physics Laboratory, Johns Hopkins University, 8621 Georgia Avenue, Silver Spring, Maryland	
Attention H. A. Tellman, Technical Liaison Representative	1

	Copies
University of Illinois, Urbana, Illinois, 306E Talbot Laboratory Attention Professor Will J. Worley	1
General Electric Research Laboratories, The Knolls, Schenectady, New York Attention H. M. Ogle	1
General Electric Company, 1 River Road, Schenectady, New York Attention V. J. Louden, Building 28-518	1
General Electric Company, Electronics Division, Advanced Elec tronics Center at Cornell University, Ithaca, New York Attention George M. Miller, Airborne Systems Section	1
Bendix Aviation Corporation, Red Bank Division, Eatontown, New Jersey Attention William H. Strasener	1
Bendix Aviation Corporation, Bendix Products Division, Mishawaha, Indiana Attention P. E. Swisher	1
Bendix Products Division, Bendix Aviation Corporation, 401 Bendix Drive, South Bend, Indiana Attention Lyle Martin, Department 863	1
Bendix Aviation Corporation, Friez Instrument Division, 1400 Taylor Avenue, Baltimore 4, Maryland Attention E. Sion, Project Engineer	1
Bendix Aviation Corporation, Bendix Computer Division, Hawthorne, California Attention Mr. C. B. Dennis, Customer Relations	1
Bendix Research Laboratory, 4855 Fourth Street, Detroit, Michigan Attention Dr. Albert C. Hall, Director of Research	1
Raytheon Manufacturing Company, 148 California Street, Newton 58, Massachusetts Attention M. S. Hartley	1
Raytheon Manufacturing Company, Missile and Radar Division, Waltham, Massachusetts Attention Mr. Harold Asquith	1
Raytheon Television and Radio Corporation, 4132 West Belmont Avenue, Chicago 41, Illinois Attention Herbert F. Wischnia, Research and Development Division	1

	Copies
Components and Materials Branch, Squier Signal Laboratory, Fort Monmouth, New Jersey Attention Mr. Marcel P. Zucchino, C.P. Section	1
Westinghouse Electric Corporation, 7325 Pennsylvania Avenue, Pittsburgh 8, Pennsylvania Attention Dr. R. A. Ramey	1
Westinghouse Electric Corporation, Friendship Airport, Baltimore, Maryland Attention Air Arm Division	1
Ahrendt Instrument Company, 4910 Calvert Road, College Park, Maryland Attention G. A. Etzweiler	1
Kearfott Company, Inc., 1150 McBride Avenue, Little Falls, New Jersey Attention J. A. Bronson	1
Convair G. M. D., Computer Group, Pomona, California Attention E. V. Mason	1
Convair, Electronics and Guidance Section, San Diego, California Attention R. T. Silberman	1
Ketay Manufacturing Corporation, 555 Broadway, New York 12, New York Attention Mr. Leo Botwin	1
Radio Corporation of America, RCA Victor Division, Camden, New Jersey Attention H. M. Roseman	1
Burroughs Adding Machine Company, 511 N. Broad Street, Philadelphia 23, Pennsylvania Attention Dr. Williamson, Research Division	1
Bell Telephone Laboratories, Whippany, New Jersey Attention L. W. Stammerjohn	1
Control Engineering Company, 560 Providence Highway, Norwood, Massachusetts Attention B. M. Hildebrandt	1
Norden Laboratories, Inc., 121 Westmoreland Avenue, White Plains, New York Attention W. J. Brachman	1
Ford Instrument Company, 31-10 Thomson Avenue, Long Island City 1, New York Attention H. F. McKinney	1

	Copies
Specialties, Inc., Skunk's Misery Road, Syosset, Long Island, New York Attention Gerard E. Forrest	1
Magnavox Company, Bueter Road, Fort Wayne, Indiana Attention A. E. Schmid, Magnetic Devices	1
Regulator Equipment Corporation, 55 MacQuester Parkway South, Mount Vernon, New York Attention W. J. Dornhoefer, Chief Engineer	1
Wayne Engineering Research Institute, 655 Merrick Avenue, Detroit 2, Michigan Attention James R. Walker	1
Radiomarine Corporation of America, 75 Varick Street, New York 13, New York	1
Philco Corporation, Philadelphia, Pennsylvania Attention R. V. Attarian	1
Davies Laboratories, 4705 Queensbury Road, Riverdale, Maryland Attention James E. King	1
Federal Telephone and Radio Corporation, 100 Kingsland Road, Clifton, New Jersey Attention W. L. Wescoat	1
Freed Transformer Company, Inc., 1713 Weirfield Street, Ridgewood, Brooklyn 27, New York Attention Philip Forman	1
Franklin Control Corporation, 1975 S. Allis Street, Milwaukee 7, Wisconsin Attention F. S. Malick	1
Engineering Department, A. C. Spark Plug Division, General Motors Corporation, Milwaukee, Wisconsin Attention D. C. Fleming	1
Control Instrument Company, Inc., 67 Thirty-fifth Street, Brooklyn 32, New York Attention Edward Lohse, Chief Development Engineer	1
Polytechnic Research and Development Company, Inc., 202 Tillary Street, Brooklyn 1, New York Attention Mr. David Feldman	1
Avco Manufacturing Corporation, Crosley Division, Cincinnati 25, Ohio Attention Lewis M. Clement, Technical Advisor to General Manager	1

	Copies
Electrical Engineering Department, Royal Aircraft Establishment, Farnborough, Hants, England Attention Dr. C. S. Hudson	1
Magnetics, Inc., E. Butler, Pennsylvania Attention E. V. Weir	1
International Instrument, Inc., 2032 Harold Street, Houston, Texas Attention H. M. Zenor	1
Fenwall, Inc., Ashland, Massachusetts Attention M. G. Freed, Project Engineer	1
General Radio Company, 275 Massachusetts Avenue, Cambridge 39, Massachusetts Attention W. N. Tuttle, Engineering Consultant	1
North American Aviation, Inc., 12214 Lakewood Boulevard, Downey, California Attention Dr. Alfred Krausz	1
Schlumberger Well Surveying Corporation, P. O. Box 2175, Houston, Texas Attention W. B. Steward, Administrative Assistant	1
U. S. Geological Survey, Section of Geochemistry and Petrology, Washington 25, D. C. Attention Leonard Shapiro, Chemist	1
Sandia Corporation, Sandia Base, Albuquerque, New Mexico Attention Allen Wooten	1
Division 1264	1
Collins Radio Company, Cedar Rapids, Iowa Attention R. F. Pickering, Engineering Department 2	1
Cook Research Laboratories, 2700 Southport Avenue, Chicago 14, Illinois Attention Donald C. McDonald	1
Chicago Midway Laboratories, 6040 Greenwood Avenue, Chicago 37, Illinois Attention Darwin Krucoff	1
Allen-Bradley Company, Milwaukee 4, Wisconsin Attention H. M. Schlicke, Consulting Engineer	1
Thompson Products, Inc., New Devices, 2196 Clarkwood Road, Cleveland 3, Ohio Attention Stephen H. Fairweather, Staff Research and Development	1

Copies

Consolidated Gas, Electric Light and Power Company of Baltimore,
385 Lexington Building, Annex 2, Baltimore 3, Maryland
Attention Library 1

Commanding Officer, U. S. Naval Ordnance Test Station, China Lake,
California
Attention Harold W. Rosenburg, Code 3542 1

Emerson Research Laboratories, 701 Lamont Street, N.W.,
Washington 10, D. C.
Attention Dr. Harold Goldberg, Director 1